

Introduction of the CDEX experiment

Ke-Jun KANG¹, Jian-Ping CHENG¹, Jin LI¹, Yuan-Jing LI¹, Qian YUE¹, Yang BAI³, Yong BI⁵, Jian-Ping CHANG¹, Nan CHEN¹, Ning Chen¹, Qing-Hao CHEN¹, Yun-Hua CHEN⁶, Zhi DENG¹, Qiang DU¹, Hui GONG¹, Xi-Qing HAO¹, Hong-Jian HE¹, Qing-Ju HE¹, Xin-Hui HU³, Han-Xiong HUANG², Hao JIANG¹, Jian-Min LI¹, Xia LI², Xin-Ying LI³, Xue-Qian LI^{3,1}, Yu-Lan LI¹, Shu-Kui LIU⁵, Ya-Bin LIU¹, Lan-Chun Lü¹, Hao MA¹, Jian-Qiang QIN¹, Jie REN², Jing Ren¹, Xi-Chao RUAN², Man-Bin SHEN⁶, Jian SU¹, Chang-Jian TANG⁵, Zhen-Yu TANG⁵, Ji-Min WANG⁶, Qing WANG^{1,1}, Xu-Feng Wang¹, Shi-Yong WU⁶, Yu-Cheng WU¹, Zhong-Zhi Xianyu¹, Hao-Yang XING⁵, Xun-Jie Xu¹, Yin XU³, Tao XUE¹, Li-Tao YANG¹, Nan YI¹, Hao YU¹, Chun-Xu YU³, Xiong-Hui ZENG⁶, Zhi ZENG¹, Lan ZHANG⁴, Guang-Hua ZHANG⁶, Ming-Gang ZHAO³, Su-Ning ZHONG³, Jin ZHOU⁶, Zu-Ying ZHOU², Jing-Jun ZHU⁵, Wei-Bin ZHU⁴, Xue-Zhou ZHU¹, Zhong-Hua ZHU⁶

(CDEX Collaboration)

¹Tsinghua University, Beijing, China 100084

²Institute Of Atomic Energy, Beijing, China, 102413

³Nankai University, Tianjin, China, 300071

⁴NUCTECH company, Beijing, China, 100084

⁵Sichuan University, Chengdu, China, 610065

⁶Yalongjiang Hydropower Development Company, Chengdu, China, 627450

Abstract

Weakly Interacting Massive Particles (WIMPs) are the candidates of dark matter in our universe. Up to now any direct interaction of WIMP with nuclei has not been observed yet. The exclusion limits of the spin-independent cross section of WIMP-nucleon which have been experimentally obtained is about 10^{-7} pb at high mass region and only 10^{-5} pb at low mass region. China Jin-Ping underground laboratory CJPL is the deepest underground lab in the world and provides a very promising environment for direct observation of dark matter. The China Dark Matter Experiment (CDEX) experiment is going to directly detect the WIMP flux with high sensitivity in the low mass region. Both CJPL and CDEX have achieved a remarkable progress in recent two years. The CDEX employs a point-contact germanium semi-conductor detector PCGe whose detection threshold is less than 300 eV. We report the measurement results of Muon flux, monitoring of radioactivity and Radon concentration carried out in CJPL, as well describe the structure and performance of the 1 kg PCGe detector CDEX-1 and 10kg detector array CDEX-10 including the detectors, electronics, shielding and cooling systems. Finally we discuss the physics goals of the CDEX-1, CDEX-10 and the future CDEX-1T detectors.

I. INTRODUCTION

Discovery of dark matter undoubtedly was one of the greatest scientific events of the 20th century, then directly searching for dark matter and identifying it will be the most important and challengeable task of this century.

As a matter of fact, the conjecture about existence of dark matter was proposed quite a long time ago in 1933 by Zwicky [1] to explain the anomalously large velocity of test stars near the Coma star astronomically observed at that

¹ corresponding author.

E-mail addresses: lixq@nankai.edu.cn(Xue-Qian Li), wangq@mail.tsinghua.edu.cn(Qing WANG)

time. The astronomical observation shows that the rotational curves of the test stars in the galaxy did not obey the gravitational law if only the luminous matter which clusters at the center of the galaxy existed. Namely, the velocities of test stars were supposed to be inversely proportional to square roots of their distances from the center of the galaxy, instead, the rotational curve turns flat. It implies that there must be some unseen matter in the galaxy, i.e. the dark matter. Moreover, hints about existence of dark matter also appear when a collision of two clusters was observed. It was observed that the center of mass of each cluster does not coincide with its center of the luminous matter after a collision between two clusters. It is explained as that two clusters both of which are composed of dark matter and luminous matter, collide, after collisions, the dark components penetrate each other because they do not participate in electromagnetic interaction (EM) neither strong interaction, but the luminous fractions of the two clusters interact with each other via EM interaction, so remain near the collision region while the dark parts left.

Moreover, all astronomical observations confirm that our universe is approximately flat, i.e. the total Ω defined as ρ/ρ_c where ρ_c is the critical density and ρ is the matter density in our universe, is close to unity. However, observation also indicates that the fraction of luminous baryonic density Ω_m is less than 4%. By fitting the observational data, it is confirmed that over 96% of matter is dark. Further analysis indicates that the dark matter may take a fraction of 24% while the dark energy occupies the rest over 72%. The dark energy is the most mysterious subject for which so far our understanding of the universe is not enough to give a reasonable answer even though there are many plausible models. By contrary, the dark matter may have a particle correspondence.

Commonly accepted point of view [2] is that the main fraction of the dark matter in our universe is the cold dark matter, i.e. the weakly-interacting-massive-particles (WIMPs). The criteria of being a dark matter candidate are that the particle does not participate in EM interaction (so it is dark!), namely it must be neutral both electric and color) and does not possess inner structure, otherwise it may have intrinsic anomalous magnetic moments and interact with EM field. Thus generally, it is the so called elementary particles. The most favorable candidate of the WIMPs is the neutralino [3], even though one cannot exclude other possibilities at the present [4, 5]. For example, He et al. [?] proposed that a scalar particle darkon can be a possible dark matter candidate which interacts with detector matter via exchange of Higgs boson. Besides, the technicolor meson [7], asymmetric mirror dark matter [8], new particles in the little Higgs model [9] as well as many other candidates have also been predicted by various models as the dark matter candidates. It is interesting that, thanks to the LHC which has already successfully been operating, one may search for such beyond standard model particles at accelerators.

One of the main goals of the detection of the dark matter is to help finding and identifying the dark matter particle(s).

To realize the task, one should design sort of experiments. Detection of dark matter is by no means a trivial job. It can be classified into the direct and indirect detections. For the first one, we should set an underground detector and try to catch the dark matter flux from outside space. In this scheme it is supposed that the dark matter flux comes from outer space, such as the halo of galaxy or even the sun and the dark matter particles (WIMPs) weakly interact with the standard model (SM) matter (mainly quarks). However, we really do not have a solid knowledge to guarantee that the dark matter particles indeed weakly interact with the regular matter as described by the gauge theory. It is just like that a black cat is confined in a dark room where there is no light, and we are supposed to catch it. Even though the chance of catching it is slim, we still have probability to get it. But if it does not exist in the room, no matter how hard we strive, we can never succeed². Therefore, generally our project of directly detecting the dark matter flux is based on such hypothesis that it does interact with the detector matter via weak interaction.

Another line is indirect detection of dark matter. In that scheme, it is hypothesized that the dark matter particle may decay or annihilate into SM particles via collisions among dark matter particles. This proposal is to explain the peculiar phenomena of e^+ excess [10] and the cosmic-ray energy spectrum [11] observed by the earth laboratories and satellites.

The China Dark Matter Experiment (CDEX) is designed to directly detect the dark matter with the highly pure germanium detector, thus later in this work we will concentrate ourselves on the discussion of direct search for dark matter. Unfortunately, the kinetic energy of the dark matter particle $\frac{1}{2}m\beta^2$ is rather low, generally the velocity of the WIMPs is $200 \sim 1000$ km/s and the value of $\beta = v/c$ is about $10^{-3} \sim 10^{-2}$, thus for a WIMP particle of 50 GeV, its kinetic energy is only a few tens of keV, which is too small to cause an inelastic transition for the nucleus (not exactly, see below discussions). When the WIMPs hit on the nucleus in the detector material, the impact makes the nucleus to recoil and then the atom would be ionized. When the nucleus is recombined with the electron clouds, photons may be radiated accompanied by the electric and thermal signals which can be detected by sensitive detectors. Each detector may be designed to be sensitive to one or a few of the signals and then record them to be analyzed off-line.

Recently, several groups have reported limited success for detecting dark matter flux. The DAMA [12] reported

² This is a story presented by Prof. T. Han at a Jin-Ping conference on dark matter detection, Sichuan, China, 2011.

their observation of the annual modulation signal and then CoGeNT [13] observed several cosmogenic peaks and their results are consistent with the DAMA's. The CDMS group reported to observe a few events of dark matter flux [?] and recently CRESST-II published their new observation results[58] and numerous underground laboratories are working hard to search for the signals of dark matter. With its special advantages, such as the thickest rock covering which can shield out most of the cosmic rays and convenient transportation and comfortable working and living condition, the Jin-Ping underground laboratory would provide an ideal circumstance for the dark matter detection and the new CDEX collaboration has joined the club for direct dark matter search. The detailed descriptions about the CDEX project will be given in the following sections.

The detection is carried out via collisions between WIMPs and nuclei. To extract any information about the fundamental interaction (SUSY, technicolor, darkon or even little Higgs etc.) from the data, much theoretical work and careful analysis must be done. For the theoretical preparation, one has to divide the whole process into three stages. The first is to consider the elementary scattering between WIMPs and quarks or gluons inside the nucleons, from there we need to derive an effective Hamiltonian describing elastic scattering between DM particle and nucleon, then the subsequent stage is the nuclear stage. Since the kinetic energy of WIMPs is rather low and generally the elastic transition dominates, the energy absorbed by the nucleons would eventually pass to the whole nucleus which recoils as described above. But this allegation is not absolutely true. Indeed the gap between radial excitations of nucleus (the principal quantum numbers of valence nucleons change) and its ground state is rather large comparing with the available collision kinetic energy. However, if the $\mathbf{L} \cdot \mathbf{S}$ coupling is taken into account, the energy levels which were degenerate would be split and the resultant gaps between the split levels could be small and comparable with the kinetic energy of the dark matter particles, thus the collision between the dark matter particle and nucleon can induce an inelastic transition and radiate photons. But this is not our concern for the CDEX project.

The highly pure germanium detector is designed to be sensitive to low energy dark matter flux.

The interaction can also be categorized into spin-independent and spin-dependent ones. So far, the measurements on the spin-independent WIMP-nucleon cross section can reach an accuracy to 10^{-44} cm^2 , but for the spin-dependent case, it is only about 10^{-39} cm^2 . It is believed that beyond 10^{-46} cm^2 , the cosmic neutrino would compose unavoidable background and the measurements do not make any sense after all.

II. A BRIEF REVIEW OF THEORETICAL FRAMEWORK FOR DETECTION OF DARK MATTER FLUX

A. Kinematics

We are dealing with collisions between WIMPs and nucleus, let us first present the necessary expressions which are related to the detection.

The recoil energy of the nucleus is [8]

$$Q = \frac{1}{2}mv^2 = \frac{2mM}{(m+M)^2}(1 - \cos\theta_{cm}) = \mu_{red}^2v^2(1 - \cos\theta_{cm}), \quad (1)$$

where m , M stand for the masses of the WIMP and nucleus, v is the absolute value of the velocity of the WIMP in the laboratory frame, μ_{red} is the reduced mass of the WIMP and nucleus and θ_{cm} is the scattering angle in the center of mass frame of the WIMP and nucleus. The recoil momentum is

$$|\mathbf{q}|^2 = 2\mu_{red}^2v^2(1 - \cos\theta_{cm}). \quad (2)$$

The recoil rate per unit detector mass is

$$R = \frac{n\sigma v}{M_D} = \frac{\rho\sigma v}{mM_D}, \quad (3)$$

where ρ is the local dark matter density which is 0.3 GeV/cm^3 in the standard halo model. The differential rate is [16]

$$\frac{dR}{dQ} = 2M_D \frac{dR}{d|\mathbf{q}|^2} = \frac{2\rho}{m} \int v f(v) \frac{d\sigma}{d|\mathbf{q}|^2} (|\mathbf{q}|^2 = 0) d^3v, \quad (4)$$

where $f(v)$ is the velocity distribution function of WIMP and

$$\frac{d\sigma}{d|\mathbf{q}|^2} (|\mathbf{q}|^2 = 0) = \frac{\sigma_0}{4\mu_{red}^2v^2}, \quad (5)$$

with σ_0 being the scattering cross section at the zero momentum transfer limit. The function $f(v)$ of DM in the galactic halo is assumed to be in the Gaussian form [8] as

$$f(\mathbf{u}) = f(\mathbf{v} + \mathbf{v}_e) = \frac{1}{(\pi v_0^2)^{3/2}} e^{-\frac{\mathbf{u}^2}{v_0^2}}, \quad (6)$$

where $v_0 \sim 270$ km/s, \mathbf{v} is the velocity of the DM with respect to the detector and \mathbf{v}_e is the velocity of the earth with $v_e = v_\odot + 14.4 \cos[2\pi(t - t_0)/T]$, and $t_0 = 152$ days, $T = 1$ year which reflects the annual modulation effects. It is noted that here $f(\mathbf{u})$ is exactly $f(v)$ which we used in above expressions. The average velocity of the dark matter is 200 km/s \sim 600 km/s, the kinetic energy $\frac{1}{2}m(\frac{v}{c})^2$ is as small as 20 \sim 200 keV as $m=100$ GeV. That is the maximum energy which can be transferred to the nucleus and cause its recoil. If the dark matter particle is as light as 10 GeV, the kinetic energy is only at the order of a few hundreds of eV. The small available energy results in a small recoil energy of the nucleus and demands a high sensitivity of our detector at low energy ranges. That raises a serious requirement for the detector design and it is the goal of the CDEX. It is worth noticing that for very low mass DM candidates which are predicted by some special models, or very low recoil energy, the contribution of DM-electron scattering is not negligible, moreover, the recoil of electron may compose the main signal[20].

B. Cross section and amplitude

The calculation of the cross section of the collision between the DM particle and nucleus can be divided into three stages: the first one is calculating the amplitudes of the elementary collision with quarks, the second stage is calculating the amplitudes for collision with the nucleon (proton and neutron), then the third stage is calculating the cross section for collision with the whole nucleus if one can assume that the nucleus is free. But in fact it is bound on lattice of crystals, thus when the small temperature effects are concerned a fourth stage calculation is required.

The WIMP particle interacts with quarks or gluons inside the nucleon [17, 18, 21, 22]. Gluons in the hadron do not participate in the weak interaction at the leading order, so that the fundamental processes concern only the interaction between DM particle and quarks. At the second stage, one needs to write up the effective Hamiltonian for the interaction between the DM particle and nucleon from the fundamental interaction. Because it is an elastic process, the nucleon remains unchanged after the collision and the total exchanged energy is transformed into the kinetic energy of the nucleon. Obtaining the effective Hamiltonian for the DM particle-nucleon interaction is by no means trivial. We will discuss the procedure more explicitly when we talk about the SI and SD processes in next subsections. Generally the collisions between dark matter particles with nucleus are very low energy processes, nucleus cannot be excited to higher radial states, thus the processes are elastic. Indeed, there might be orbital excitations and the collision would be inelastic, in general such processes only cause very small observable effects. Later the excited nucleus radiates a photon and returns to the ground state, but for the germanium detector which cannot detect photon radiation, such effects do not need to be considered. We only concentrate on the nucleus recoil effects. Definitely, the goal of the whole research is to identify the DM particle(s) and discover the interaction which may be new physics beyond the standard model. But for this purpose, we need to study the observable effects and learn how to extract useful information about the fundamental processes.

The cross section between WIMP and nucleus is

$$\sigma = \frac{1}{mMv} \frac{1}{(2s_1 + 1)(2s_2 + 1)} \sum \int \frac{d^3p'_1}{(2\pi)^3} \frac{1}{2E'_1} \frac{d^3p'_2}{(2\pi)^3} \frac{1}{2E'_2} |M|^2 (2\pi)^4 \delta(p_1 + p_2 - p'_1 - p'_2),$$

where v is the velocity of the DM particle while the nucleus is assumed to be at rest before collision, p_1, p_2, p'_1, p'_2 are the momenta of the DM particle and nucleus in the initial and final states respectively, s_1, s_2 are the spins of the DM particle and nucleus, the sum is over all the polarizations of the outgoing DM particle and nucleus, M is the collision amplitude which is what we need to calculate.

How to get the effective coupling of $DM - N\bar{N}$ depends on the concrete model adopted in the calculation [17, 18, 23, 24]. For example, the exchanged meson between the DM particle and nucleon could be the SM Z^0 or Higgs boson [19], whereas in the models beyond the standard model the exchanged agents may be Z' or others.

1. Amplitude

The elementary process is an elastic scattering between the DM particle and quarks. For example in the standard model (SM) the exchanged boson between DM particle and quark (u,d,s) is Z^0 or Higgs boson whereas in the new

physics beyond the SM, it may be Z' etc. The Lagrangian which is determined by the pre-postulated models of the dark matter and the effective interaction is written as

$$\mathcal{L} = l_\Gamma \bar{q} \Gamma q \quad (q = u, d, s), \quad (7)$$

where Γ is a combination of the γ matrices ($S, \gamma_\mu, i\sigma_{\mu\nu}, \gamma_\mu\gamma_5, \gamma_5$) and transfer momentum q , l_Γ is the corresponding DM current. It is noted that only the scalar S and axial vector $\gamma_\mu\gamma_5$ do not suffer a suppression of smaller transfer momenta. The former corresponds to the SI process which will be discussed in next subsection and the later one is proportional to the quark spin under the non-relativistic approximation and results in the spin-dependent (SD) cross section.

According to the general principle of the quantum field theory, the amplitude of the elastic scattering between the dark matter particle with a single nucleon should be written in the momentum space because during the process the total energy and the three-momentum are conserved. Thus the amplitude is

$$M = l_\mu \bar{u}(\mathbf{p}', s'_z) J^\mu u(\mathbf{p}, s_z), \quad (8)$$

where l_μ is the DM current, $\mathbf{p}, \mathbf{p}', s_z, s'_z$ are the three-momenta and spin projections of the initial and final states of the nucleon and J^μ is the corresponding nucleon current of the effective interaction (for such as the darkon models, J^μ would be replaced by a scalar, for more complicated models, it might even be tensors). If the nucleon is free, the amplitude can be easily calculated as depicted in any textbook of quantum field theory. However the nucleon is not free but bound in the nucleus, thus the wavefunction which describes the state of the nucleon is a solution of the Schrödinger equation with very complicated nuclear potential, such as the Paris potential, written in the coordinate space. Thus, one needs to derive the formula in terms of the given wavefunctions via a Fourier transformation.

$$\begin{aligned} M &= l_\mu \bar{u}(\mathbf{p}', s'_z) J^\mu u(\mathbf{p}, s_z) \\ &= l_\mu \frac{1}{(2\pi)^3} \int d^3x' e^{-i\mathbf{p}'\cdot\mathbf{x}'} \bar{u}(\mathbf{x}', s'_z) J^\mu \frac{1}{(2\pi)^3} \int d^3x e^{i\mathbf{p}\cdot\mathbf{x}} u(\mathbf{x}, s_z) \times (2\pi)^3 \delta(\mathbf{x}' - \mathbf{x}) \\ &= l_\mu \frac{1}{(2\pi)^3} \int d^3x e^{-i(\mathbf{p}' - \mathbf{p})\cdot\mathbf{x}} \bar{u}(\mathbf{x}, s'_z) J^\mu u(\mathbf{x}, s_z) \\ &= l_\mu \frac{1}{(2\pi)^3} \int d^3x e^{-i\mathbf{q}\cdot\mathbf{x}} \bar{u}(\mathbf{x}, s'_z) J^\mu u(\mathbf{x}, s_z), \end{aligned} \quad (9)$$

where $\bar{u}(\mathbf{x}, s'_z), u(\mathbf{x}, s_z)$ are the wave functions of the nucleon in the coordinate space. The delta function $(2\pi)^3 \delta(\mathbf{x}' - \mathbf{x})$ is introduced because the interaction occurs at the same point (i.e. the propagator is reduced as $\frac{1}{q^2 - M^2} \approx \frac{-1}{M^2}$ where M is the mass of the medium boson which is heavy and M^2 is much larger than q^2). Now let us step forward to discuss the scattering amplitude between the DM particle and nucleus. We re-interpret the wave function $u(x, t)$ in the above expression as the corresponding field operator in the second quantization scheme. The nucleon field operator $\Psi_N(\mathbf{r}, t)$ can be written as

$$\Psi_N(\mathbf{r}, t) = \sum_\alpha [a_\alpha u_\alpha(\mathbf{r}) e^{-iE_\alpha t} + b_\alpha^\dagger \nu_\alpha(\mathbf{r}) e^{iE_\alpha t}]. \quad (10)$$

where a_α and b_α^\dagger are annihilation and creation operators of baryon and anti-baryon. The probability operator of the nucleon density at \mathbf{r} is

$$\Psi_N^\dagger(\mathbf{r}, t) \Psi_N(\mathbf{r}, t). \quad (11)$$

The nuclear ground state can be expressed as

$$|\Psi_A \rangle = e^{i\mathbf{P}\cdot\mathbf{X}} (\prod_{i=1}^A a_i^\dagger) |0 \rangle,$$

where $|0 \rangle$ is the vacuum, A is the number of nucleons in the nucleus and the product corresponds to creating A nucleons (protons and neutrons) which are the energy eigenstates. The phase factor $e^{i\mathbf{P}\cdot\mathbf{X}}$ corresponds to the degree of freedom of the mass center of the nucleus, where \mathbf{P} is the total momentum of the nucleus and \mathbf{X} is the coordinate of the mass center of the nucleus. In the center of mass frame, $\mathbf{P} = 0$, the phase factor does not show up. Indeed, the phase factor only corresponds to a free nucleus, instead, if one further considers that the nucleus is bound on the lattice of crystal such as germanium, the phase factor would be replaced by a complicated function. Unless we discuss the thermal effect such as for the CDMS detector, the nucleus can be treated as a free particle without causing much errors. The thermal effect can be calculated in terms of the phonon theory. However, in most cases, the nucleus can be treated as a free particle, and a simple phase factor sufficiently describes this degree of freedom.

Sandwiching the probability operator Eq. (8) between the nuclear ground state, we have

$$\int d^3x e^{i\mathbf{q}\cdot\mathbf{x}} \langle 0 | e^{-i\mathbf{P}'\cdot\mathbf{X}} (\prod_{i=1}^A a_i) \sum_{\alpha\beta} a_\alpha^\dagger \bar{u}_\alpha(\mathbf{x}) e^{i\omega_\alpha t} (J^\mu) a_\beta^\dagger u_\beta(\mathbf{x}) e^{-i\omega_\beta t} (\prod_{i=1}^A a_i^\dagger) e^{i\mathbf{P}\cdot\mathbf{X}} | 0 \rangle. \quad (12)$$

Now, let us turn to the laboratory reference frame where the recoil of the nucleus must be clearly described. By doing so, we need to consider the phase factor $e^{i\mathbf{P}\cdot\mathbf{X}}$ in Eq.(14). As aforementioned the scattering between the DM particle and nucleus is elastic, thus any single nucleon cannot transit from its original state to an excited state, but transfers its kinetic energy gained from the collision with the DM particle to the whole nucleus. The practical process of the energy transfer is via interaction among all the nucleons in the nucleus, so must be very complicated. Fortunately, we do not need to know all details of the process. Since the inner state of the nucleus does not change after the collision, the wavefunction of the nucleus can only vary by a phase factor. We consider that the time duration of the energy transfer process is very short compared with our measurement, we may use the "impulse" approximation, i.e. the nucleus does not have enough time to move. The phase factor obviously does not depend on the coordinates of any individual nucleon, so can only be related to the coordinate of the mass center of the nucleus \mathbf{X} . Including this phase factor, we would rewrite the expression (14) as

$$\begin{aligned} & \int d^3X \langle 0 | e^{-i\mathbf{P}'\cdot\mathbf{X}} e^{-i\mathbf{q}\cdot\mathbf{X}} \int d^3x (\prod_{i=1}^A a_i) \sum_{\alpha\beta} a_\alpha \bar{u}_\alpha e^{i\omega_\alpha t} (J^\mu) a_\beta^\dagger u_\beta e^{-i\omega_\beta t} e^{-i(\mathbf{p}_\alpha\cdot\mathbf{x}_\alpha - \mathbf{p}'_\beta\cdot\mathbf{x}'_\beta)} (\prod_{i=1}^A a_i^\dagger) e^{i\mathbf{P}\cdot\mathbf{X}} | 0 \rangle \\ & = (2\pi)^3 \delta(\mathbf{P} - \mathbf{P}' - \mathbf{q}) \int d^3x \langle 0 | (\prod_{i=1}^A a_i) \sum_{\alpha\beta} a_\alpha \bar{u}_\alpha e^{i\omega_\alpha t} (J^\mu) a_\beta^\dagger u_\beta e^{-i\omega_\beta t} (\prod_{i=1}^A a_i^\dagger) e^{-i(\mathbf{q}\cdot\mathbf{x})} | 0 \rangle, \end{aligned} \quad (13)$$

where the δ -function explicitly embodies the momentum conservation. For simplicity, below, we will not show this factor anymore, as well understood. It is shown that for elastic scattering $\alpha = \beta$, so the factor $e^{-i\omega_\beta t} e^{i\omega_\alpha t} = 1$, but if, as aforementioned, there exists orbital excitation, this factor is no longer 1, but in general cases, it is indeed very close to unity.

There are two types of cross sections : the SI- spin-independent and SD- spin-dependent ones.

2. The SI cross section

The fundamental interaction between the DM particle and quarks is gained based on models, various models would result in different Hamiltonian. Nevertheless, from the fundamental interaction between the DM particle and quarks to the level of nucleons, the procedure was explicitly demonstrated in Refs.[6, 19, 27], and the readers are suggested to refer to those enlightening works.

As noted, if the interaction between the DM particle and quarks is spin-independent, for example the darkon case [6], the particle interaction and the nuclear effect can be factorized and an enhancement factor proportional to A appears.

The observation rates for spin-independent scattering can be written as [16]

$$\frac{d\sigma}{d|\mathbf{q}|^2} = G_F^2 \frac{C}{v^2} F^2(|\mathbf{q}|) = \frac{\sigma_0}{4m_r^2 v^2} F^2(|\mathbf{q}|), \quad (14)$$

where G_F is the universal Fermi coupling constant, σ_0 is the cross section at zero-recoil, m_r is the reduced mass of the WIMP and nucleus, finally $F(|\mathbf{q}|)$ is the nuclear form factor. Generally speaking, the mass density distribution of the nucleus is proportional to the charge density or the nucleon number density, hence the form factor can also be accounted from the nucleon number density in the nucleus, i.e. the nuclear density. The most general form is given in Eq. (14), but for the SI cross section, the recoil effect can be attributed into a simple form factor. The form factor is the Fourier transformation of the nuclear density as

$$\begin{aligned} F(q) & = \frac{1}{A} \int \rho(r) e^{-i\mathbf{q}\cdot\mathbf{r}} d^3r \\ & = \frac{4\pi}{A} \int \frac{r}{q} \rho(r) \sin(qr) dr, \end{aligned} \quad (15)$$

where $\rho(r)$ is the nuclear density. Here we assume that the nucleus is spherically symmetric and it is only a function of r . Obviously, unless one can more accurately determine $F(q)$, extraction of useful information from data is impossible.

There are several ansatz for determining the form factor by assuming typical $\rho(r)$ functions [28–31].

The form factor $F(q)$ is required to obey

$$F(0) = 1.$$

The numerical results show [32] that the form factors determined by the various models for the nuclear density do not deviate much from each other, therefore for not very high accuracy of measurement, one can use either of the models.

Generally, the SI cross section can be written as

$$\sigma_0^{SI} = \frac{4}{\pi} m_r^2 [Z f_p + (A - Z) f_n]^2, \quad (16)$$

and eventually we have

$$\frac{dR}{dQ^2} = \frac{\rho_0 \sigma_0}{2m_\chi m_r^2} F(Q)^2 \int_{v_{min}}^{v_{max}} \frac{f(v)}{v} dv, \quad (17)$$

where $Q^2 = -q^2$ in the time-like form. Here f_p and f_n are related to the proton and neutron respectively which can be derived from the given effective couplings between DM particle and nucleon discussed above. To a good approximation

$$f_n \approx f_p, \quad (18)$$

thus $\sigma_0^{SI} \propto A^2$ is a large enhancement factor, especially for heavy nuclei. Therefore, thanks to the enhancement factor, the total spin-independent cross section could be much larger than the cross section for DM particle scattering with single nucleons. That is why, the present data can reach an accuracy of 10^{-44} cm² for SI cross section between DM and nucleon.

3. The SD cross section

For the elastic scattering with small momentum transfer, the contribution of the axial vector is dominant

$$g^2 l^\mu \bar{q} \gamma_\mu \gamma_5 q \approx g^2 \mathbf{1} \cdot \bar{q} \mathbf{s} q, \quad (q = u, d, s), \quad (19)$$

where g is the coupling in the concerned theory and l^μ is the leptonic current (could be vector and/or axial vector). Summing over the contributions of all partonic spin projections, one would step to the interaction between the DM particle and nucleon. Thus the effective current for nucleon is [25, 26]

$$\langle p(n) | \sum_{u,d,s} g \bar{q} s_z q | p(n) \rangle = \sum_{q=u,d,s} A_q^{p(n)} \Delta_q, \quad (20)$$

where $\Delta_q \equiv s_q(\uparrow) - s_q(\downarrow) + \bar{s}_q(\uparrow) - \bar{s}_q(\downarrow)$, A_q^p , A_q^n can be obtained from the fundamental Hamiltonian[21]. By the data, we have

$$\Delta_u^{(p)} = 0.78 \pm 0.02, \quad \Delta_d^{(p)} = -0.48 \pm 0.02, \quad \Delta_s^{(p)} = -0.15 \pm 0.02,$$

and $\Delta_u^{(n)} = \Delta_d^{(p)}$; $\Delta_d^{(n)} = \Delta_u^{(p)}$; $\Delta_s^{(n)} = \Delta_s^{(p)}$.

Calculating the SD cross section is much more complicated than that for SI cross section. For the SD process, the nuclear effect cannot be factorized out, but entangled with the fundamental sub-processes.

The unsuppressed effective nucleon current is [33, 34]

$$\langle p, s | \mathcal{J}_5^\mu(x) | p', s' \rangle = \bar{u}_N(p, s) \frac{1}{2} [(a_0 + a_1 \tau_3) \gamma^\mu \gamma_5 + (b_0 + b_1 \tau_3) q^\mu \gamma_5] u_N(p', s') e^{iq \cdot x} \quad (21)$$

where $q = p - p'$ and a_0, a_1 are given as

$$a_p = a_0 + a_1 = \sum_{q=u,d,s} A_q^p \Delta_q; \quad (22)$$

$$a_n = a_0 - a_1 = \sum_{q=u,d,s} A_q^n \Delta_q, \quad (23)$$

as the results of Eq.(9).

Generally, the spin-dependent cross section can be decomposed into the isoscalar S_{00} , isovector S_{11} and interference term S_{01} as

$$S_{SD}^A = a_0^2 S_{00}(q) + a_1^2 S_{11}(q) + a_0 a_1 S_{01}(q), \quad (24)$$

where a_0 , a_1 are just the coefficients of isospin 0 and 1 components of the effective current.

In fact, the amplitude for the spin-dependent collision between DM particle and nucleus is similar to that of nuclear β decay which was thoroughly studied by the nuclear physicists long time ago [35]. The calculations on the SD cross sections have been discussed by many authors [36]. Here we just outline the work given in literature which will be useful for our analysis of the data taken by the CDEX experiments.

Now let us forward to the stage of DM-nucleus. For zero-momentum transfer,

$$\bar{N}\gamma_\mu\gamma_5 N = u_N^\dagger \boldsymbol{\sigma} u_N,$$

where u_N is the simple two-component fermion spinor of nucleon. When the momentum transfer is not zero ($\mathbf{q} \neq 0$), the isovector part of the axial current induces a pseudoscalar term[33] as shown in Eq.(21). By the reduction formula of the QFT, the axial current should couple to a pseudoscalar meson, and the lightest pseudoscalar meson is the pion, so that the virtual pion would compose the most important contribution to the new term. Thus we have relations $b_0 = 0$ and $b_1 = \frac{a_1 m_N}{\mathbf{q}^2 + m_\pi^2}$ by assuming PCAC. Then under the non-relativistic approximation the matrix element (21) becomes

$$\langle p, s | \mathcal{J}_\mu^5(x) | p', s' \rangle = u_N^\dagger(p, s) \left[\frac{1}{2} (a_0 + a_1 \tau_3) \boldsymbol{\sigma} - \frac{1}{2} \frac{a_1 \boldsymbol{\sigma} \cdot \mathbf{q} \tau_3}{\mathbf{q}^2 + m_\pi^2} \mathbf{q} \right] u_N(p', s') e^{i\mathbf{q} \cdot \mathbf{x} - i\omega t} \quad (25)$$

as q_0 being zero for the elastic scattering and for very low energy inelastic scattering we still can approximate $e^{-i\omega t} \approx 1$.

The total cross section commonly is evaluated in terms of the multipole operators method [37]. Under the non-relativistic approximation, the scattering amplitude can be written as

$$\mathcal{M} = \mathbf{1} \cdot \int d^3x \langle JM | \mathcal{J} | JM' \rangle e^{i\mathbf{q} \cdot \mathbf{x}}, \quad (26)$$

thus the differential cross section reduces into

$$\frac{d\sigma}{dq^2} = \frac{G}{(2J+1)v^2} S(q), \quad (27)$$

where

$$S(q) = \sum_{L \text{ odd}} (| \langle J | \mathcal{T}_L^{el}(q) | J \rangle |^2 + | \langle J | \mathcal{L}_L(q) | J \rangle |^2), \quad (28)$$

and G is a constant depending on the model adopted for the calculation, $\mathcal{T}^{el}(q)$ and $\mathcal{L}(q)$ are the transverse and longitudinal electric projections of the axial current. The explicit expressions of $\mathcal{T}^{el}(q)$ and $\mathcal{L}_L(q)$ are defined and calculated in Refs.[25, 26, 33, 34], for saving space, we do not present them here and the readers who are interested in the details are recommended to refer the original works.

It is also noted that since the matrix elements depend on the expectation values of $\boldsymbol{\sigma}$, the contributions from the nucleons at lower energy states, in the language of the shell model, i.e. the nucleons at the inner shells, should cancel each other. In other words, the nucleons at lower states would make null contributions to the scattering matrix elements. Only a few nucleons residing on the very outer shells, the so-called valence nucleons make substantial contributions to the DM-nucleus scattering. That is why the SD cross section is much more difficult to be measured than the SI one.

It is interesting to look deeper on the SD transitions because there may occur inelastic scattering processes. As aforementioned, the gaps between the energy levels pertaining to the different principal quantum numbers are large compared to the available kinetic energy of the dark matter particle, so that the nucleon which is colliding with the DM particle cannot transit to an energy shell with higher principal quantum number. However, due to existence of the $\mathbf{L} \cdot \mathbf{S}$ coupling, the energy level ($l \neq 0$) which was degenerate would be split into two levels, and the gap between the two levels is small and completely comparable with the kinetic energy of DM particle, so that the nucleon may transit into a higher energy level after the collision and the scattering is inelastic.

Moreover, via the loop effect, the axial current Lagrangian can induce an effective scalar coupling which is SI-type and can be enhanced by the factor A^2 . Thus the effective coupling is loop-suppressed, but the total cross section is

enhanced by A^2 , so its net effect may be comparable with that of the tree contribution of the axial currents. The situation becomes more complex and needs to be carefully investigated when the data are analyzed.

Anyhow, extracting useful information from the data is by no means an easy job. Not only careful analysis on the background, but also a serious theoretical study must be carried out.

As introduced above, the accuracy for detecting the SI cross section has already reached 10^{-44} cm^2 , it is well known that if the cross section is smaller than 10^{-46} cm^2 , the contribution of the atmospheric neutrinos cannot be eliminated. Thus if to 10^{-46} cm^2 (the accuracy might be reached in a few years), the DM flux is still not observed there could be some possibilities, one is that the DM particles do not interact with the SM particles via weak interaction, and another possibility is that the DM particles are no WIMPs, but something else, for example heavy sterile neutrino etc. If it is the first, DM only participates in gravitational interaction, it would be a disaster for us because on the earth, the present available apparatus has no chance to measure gravitational effects, and in the future it is an unanswered inquiry. If it is the second, we need to do more theoretical study to explore possible channels to check the postulates.

For the SI cross section, because the Hamiltonian caused by the effective interaction does not contain a spin-operator, the spin of the nucleon cannot flip during the collision, thus the scattering is fully elastic. By contraries, for the SD cross section, the Hamiltonian contains a spin operator which may induce a spin flip, therefore the spin projection of the final state of the nucleon may be different from the initial one, namely a transition from lower energy level to higher one occurs during the collision. Obviously the nucleus is excited after the inelastic collision, then it definitely will return back to the ground state by radiating a photon. The photon should have a characteristic spectrum, which can be "seen" in a detector. The signal might be weak and detection is rather difficult as expected. This scheme would be a subject of further investigation. However, it is not applicable to our Jin-Ping project because the light signals are not detected at our germanium detector at all.

Indeed, we prey that the DM particle indeed interacts with SM quarks, then nucleons via weak interaction, so that we can find its trace through the direct search on the underground detectors, otherwise, one would be unable to identify the mysterious matter even though we know for sure of its existence.

III. REVIEW OF EXPERIMENT

A. Overview

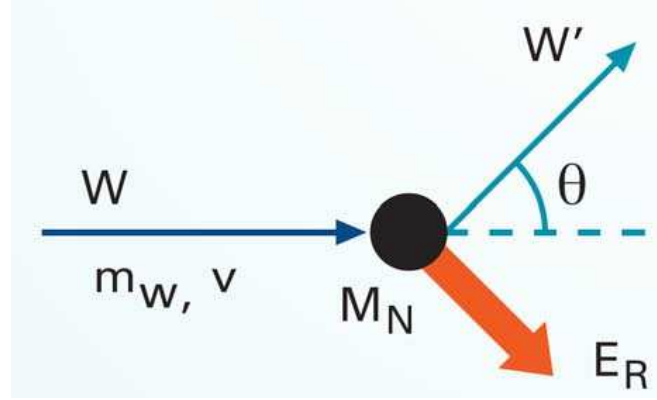
It is very important for scientists to detect dark matter particles with different experimental methods in order to understand the essence of dark matter. Usually experimental detection of dark matter can be divided into two types: direct detection and indirect detection. For indirect detection of dark matter, the SM particles, such as gammas, neutrinos, and etc., which are generated from annihilation of two dark matter particles or decays of DM particles, can be detected. The possible site for dark matter particles to annihilate each other should be the vicinity near the center of a star such as the Sun or planets including our Earth, where the gravitational force traps the dark matter particles whose density rises to a relatively high level, so that the possibility of dark matter particle annihilation there would be higher than at other places. The large-scale high-energy accelerator may also detect indirectly the dark matter particles which are generated by collisions of energetic particle beams. But since the produced dark matter particles are stable neutral bosons (might be fermions also), so they only manifest as missing energy, detecting them is a challenge to our detection technology. Instead, direct detection of dark matter particles mainly focuses on the measurement of the deposited energy of a recoiled nucleus scattered off by the coming dark matter particle, mainly the Weakly Interacting Massive Particle (WIMP). The essence of direct detection of WIMP is to single out the possible events induced by the coming dark matter particles from a large background produced outside and inside the detector system. So the ultra-low background level of the detecting system for direct detection of WIMP is a crucial requirement Fig.1.

For different detectors, the deposited energy of the recoiled nucleus scattered off by the incident WIMP in the fiducial volume of the detector usually can be detected with three different processes: ionization, scintillation and heating. So the three main types of detectors are ionization detector, scintillation detector and heating detector which measure respectively ionized electrons, scintillation light and temperature variations. Some detectors are designed to extract information from a combination of two such processes in order to improve the ability of discriminating the "real" WIMP signal from the background events.

More than tens of groups in the world now are carrying out experiments to directly detect WIMPs and the results have been achieved to the level less than 10^{-7} pb for WIMP mass of around 50 GeV.

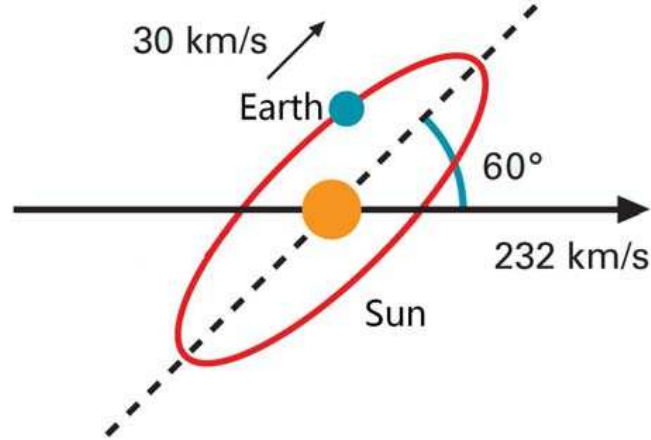
For the scintillation method, crystals such as NaI(Tl) and CsI(Tl) are used as the target detectors. Scintillation detector can provide a pulse shape to discriminate the WIMP events from background events and it is easy to produce a larger prototype detector which can be a ton-mass scale detector. Ultra-pure scintillation detectors have been studied and run for a long time to detect WIMP. The DAMA Collaboration has built its NaI scintillation crystal array detector

FIG. 1: The principle of WIMP direct detection.



with the mass scale of hundreds of kilograms [38]. The KIMS group has chosen almost the same technology with DAMA except the scintillation crystal is CsI(Tl) [39]. The relative low photoelectron yields restrict the application of the pulse shape discrimination method at low energy region. Both the DAMA and KIMS experiments turn to detect the annual modulation of the event rate induced by WIMPs(Fig.2). The DAMA Collb. has achieved an average event rate of 1cpkcd above 2 keV and given a clear annual modulation result with 1.17 ton \times yr data set and 13 annual cycles. Based on these results, the DAMA collaboration claimed that they had found evidence of dark matter.

FIG. 2: The relative velocity of the earth to the sun and the velocity of the sun moving in the WIMP "sea".



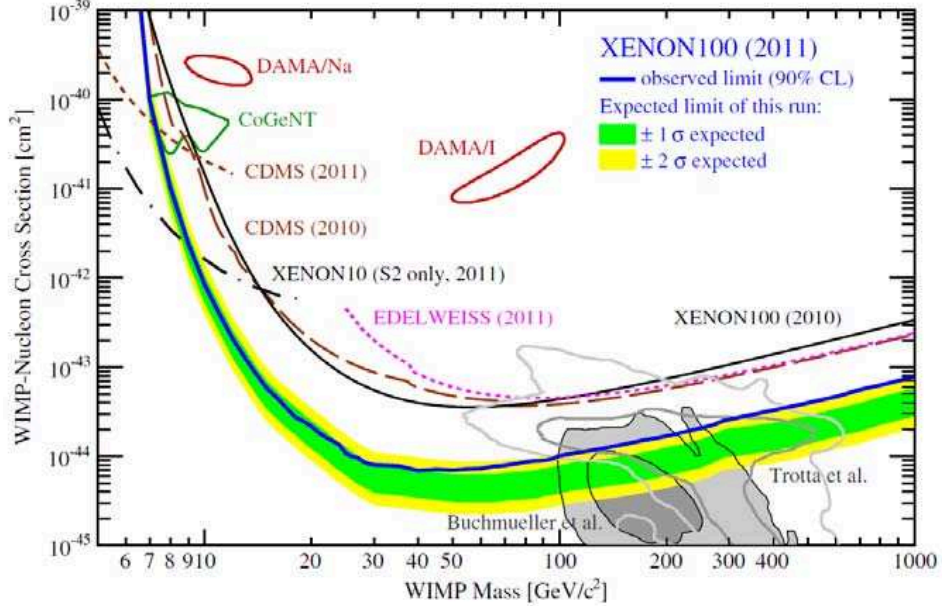
For the ionization method, high purity germanium detector is the best choice till now due to its ultra-low self-radioactivity and feasibility to develop large-scale detector technically. Germanium detector could provide low energy threshold and very good energy resolution, but its shortcoming is a not-good ability to discriminate the recoiled events induced by incident WIMPs from the background events of gamma and electron. This disadvantage limits Ge detectors or other semiconductor detectors to reach high detection accuracy for a relatively large background.

For the heating method, the detectors could measure a tiny vibration of temperature and heat deposition inside of the detector materials when the detectors run in the ultra-low temperature circumstance with only tens of millikelvin. The heat deposition can induce a change of the current signal in the equipped electronics and then will be recorded.

For dark matter search experiments, the primary and key task is to extract out possible signals from the recorded events which include a large number of background debris and determine if they are induced by the incident dark matter particles. So several experimental groups choose detectors which could simultaneously measure two kinds of signals induced by one interaction and this strategy could make the detector to possess a very strong ability to discriminate background. Now two collaborations, CDMS and XENON, have published the most stringent and sensitive results of a detection for tens of GeV-mass WIMP. The CDMS group has developed a new type of Ge and Si detector which collects both the ionization and heat signals. A kind of superconducting tungsten transition-edge sensors (TESs) has been used to read out the heat deposition, at the same time the ionization signal is also recorded.

So two kinds of signals including ionization and heat are read out when one incident particle hits the target in the fiducial volume of the detector. The ratio of the ionization energy and heat energy could be different for the recoils of the nucleus which is scattered off by WIMP and the background events caused by incident gammas and/or electrons. This scheme provides a very strong event discrimination for the CDMS experiment. The CDMS group has run its Ge and Si detecting system for several years and published its new observation result in 2010 and 2011 (Fig.??).

FIG. 3: The physical results from CDMS, XENON and other group for WIMP search.



The XENON group has also developed their liquid Xenon TPC(Time Project Chamber) detector which collects both the ionized electrons and scintillation light when a particle interacts with the xenon target. Now the XENON100 experiment has built its liquid xenon detector of 100 kg fiducial mass and published new results in 2011 [40].

B. Ultra-low energy threshold experiment

In recent years, an ultra-low energy threshold of about 400 eV has been achieved with the germanium detector based on the point-contact technology, the point-contact germanium detector PCGe is used for scanning WIMP of mass as low as 10 GeV. The scientists from Tsinghua university of China first started the experimental preparation from 2003 [41] and ran the first 5g-mass planar Ge detector for a test. The TEXONO collaboration runs a 20g ULE-HPGe detector with the shielding system on the ground near a nuclear power plant in Taiwan and published its physical results in 2009 shown in Fig.4 [42]. The CoGeNT Collaboration has also started a similar experiment for the WIMP search with 475g PCGe detector at a ground laboratory from 2006 and published its physical results in 2008 and 2011, respectively [43]. The CoGeNT experiment has explored a low WIMP mass region and its results are shown in Fig.5.

Due to the updated results from Ge detectors, the low-mass WIMP detection has become one of the new hot topics for dark matter experiments. Many groups have tried to develop lower threshold detectors to scan the low mass WIMP region below 10 GeV. The Majorana[44] and GERDA[45] groups try to reduce their energy threshold to cover the energy range for both double beta decay and dark matter search.

In 2009, the CDEX Collaboration is aiming to search for low mass WIMPs with a ton-scale point-contact germanium detector located at the Jin-Ping underground Laboratory (CJPL) in China. Now the first stage of the CDEX project-CDEX-1, where one 1kg-mass PCGe detector is installed has already successfully run and begun to take data.

IV. THE CJPL

Experiments such as detection on dark matter, double beta decay experiment and neutrino experiment in the particle physics domain require Ultra-low background laboratories in order to identify the rare events. Those deleterious

FIG. 4: The physical results of WIMP detection from TEXONO group.

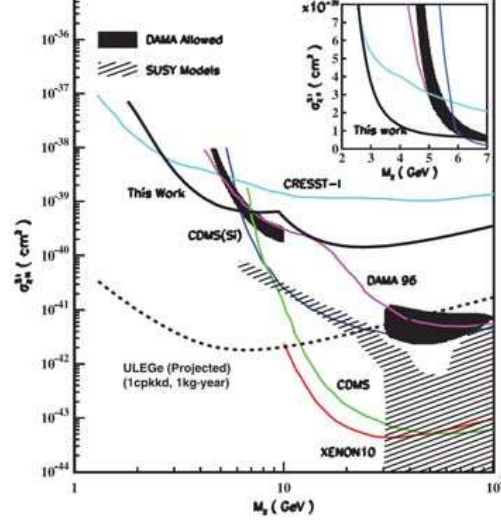
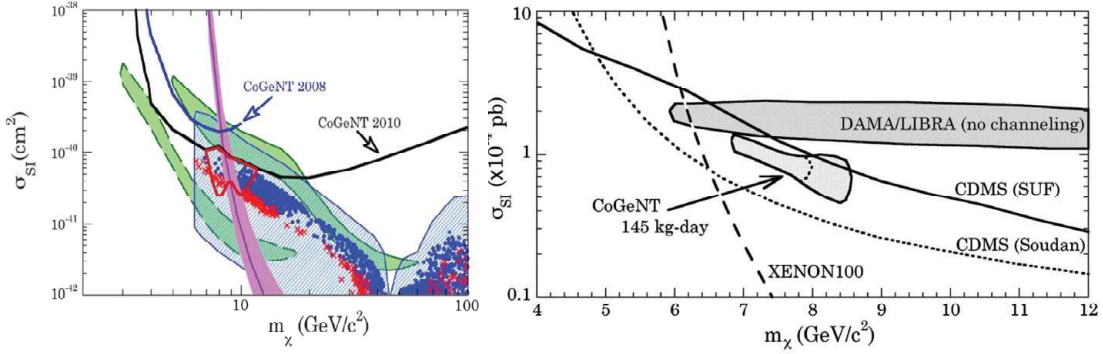


FIG. 5: The physical results of WIMP detection from CoGeNT group.



background events come mainly from the radioactive isotope of environmental materials, high energy cosmic-ray muons which originate from the interaction of high energy protons in cosmic rays with atmospheric compounds at outer space, as well as the internal backgrounds from active isotopes in detector materials and the noise of the detector electronics. The ambient radioactive background from the radioactive nuclei could be shielded with efficient shielding system which includes possible passive and active shielding parts. However the high energy muons, which are the main hard contents of cosmic-ray, can pass through the environment and interact with the shielding system materials, the structure materials and the detector itself. Though the instantaneous events coming from direct interaction of muons with those materials on their paths can be vetoed by an active muon veto system, the delayed neutron and accompanying radioactive nuclei induced by incident cosmic-ray muons can contribute to backgrounds in the detector. This channel is the most difficult one to be shielded and extracted out from the spectrum of the detection. So it is very necessary that the detection of dark matter should be performed at underground laboratories where the muon particles are efficiently stopped and absorbed by the overburden rock.

There are many underground laboratories established or under construction in the world including the LNGS in Italy, Kamioka in Japan, Sudbury in Canada, Modane in France, Soudan in USA, and so on [46]. In 2010, the first deep underground laboratory was built with excellent working and living conditions in China. This deep underground laboratory is named The China Jin-Ping Underground Laboratory (CJPL).

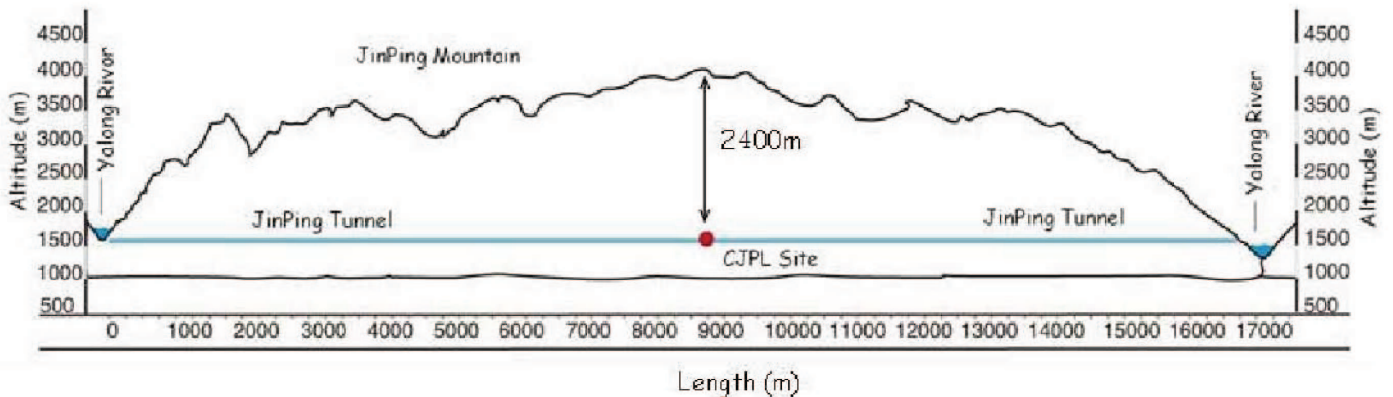
A. The CJPL environment

The Yalong River is more than 1500-km long in Sichuan province of China. A part of almost 150 km of the river bends and encompasses the huge Jin-Ping Mountain to make a narrow arc. The turning is very sharp at the turning point, namely in the mathematical terminology the curvature radius is small at the spot, thus the west and east parts of the river are not much apart, but separated by the mountain and the height difference of their water surfaces is quite large. If a tunnel is drilled from the east to the west along the intercept of the arc, the water drop height is tremendously large, so that this can serve as an ideal hydrodynamic resource. Two hydropower plants at each side of the Jin-Ping Mountain on the Yalong River are being built now by Yalong River Basin Hydropower Development Company. Totally seven parallel tunnels are drilled including one drainage tunnel, two transport tunnels and four headrace tunnels[47]. In 2008, these two transport tunnels were completed and have been in use for the hydropower plant project, and the map is shown in Fig.6. The length of these two transport tunnels is 17.5 km and the cross-section is about 6m×6m. The CJPL is located in the central portion of one of the transport tunnels and the rock overburden is about 2400 m thick. Fig.7 shows the detailed location of the CJPL in the transport tunnel and the transect profile of the transport tunnel.

FIG. 6: The site of CJPL.



FIG. 7: The cross-section of the Jin-Ping Mountain along the transportation tunnel. The site of CJPL is in the middle part of the Jin-Ping tunnel and can access by drive.



Tsinghua University, collaborating with Yalong River Basin (originally called Ertan) Hydropower Development Company who owns the Jin-Ping tunnel, had made a plan to build an underground laboratory which was large enough to host a relatively large-scale low-background experiment. The project is under way right now. As the first step, a small CJPL hall has been constructed for dark matter experiment and an ultra-low background material screening facility has also been installed. The CJPL internal space includes three parts: the entrance tunnel of 20 m in length, 30 m-long connection tunnel and the main hall with dimension of 7.5m(H) \times 6.5m(W) \times 40m(L) and the total available volume is about 4000m³. The wall of CJPL is covered by a layer of air-proof resin to separate it from the rock of the tunnel. There are a ground laboratory building, office and dormitory for the researchers near the entrance of the tunnel. Apartments, restaurants, hotel and sport facilities are also available nearby the ground laboratory.

In order to provide a good working condition with fresh air for researchers and further decrease the radon concentration in the air of the internal space, a 10-km long air ventilation pipe has been built to pump the fresh air from outside the transport tunnel into the CJPL space. This ventilation system can provide up to 2000m³/h fresh air and keep the air clean inside the CJPL. According to the need of dark matter experiment, the radon trapping system will be installed in the CJPL serving as an improved radon gas filter. The CJPL is equipped with 3G wireless network and fiber access to broad-band internet.

B. CJPL facilities

Low background germanium spectrometer serves as the standard facility for material screening and selection for either detection of dark matter or neutrinoless double beta decay experiments [48]. A low background germanium spectrometer, called GeTHU facility, with a dedicated low background shield has been designed and set up lately at CJPL for material selection of dark matter experiment CDEX and other rare-event experiments. Now the facility is operating for background measurement. Moreover, another two counting facilities are being designed to improve minimum detecting sensitivity.

The detector is a high-purity, N-type germanium detector (HPGe) with a relative efficiency of 40% and was constructed by CANBERRA in France [49]. The germanium crystal has a diameter of 59.9 mm and a thickness of 59.8 mm. The cryostat is made of ultra low background aluminum with a U shape to avoid direct line-of-sight to outside (see Fig.8(a)). The preamplifier is placed outside the shield, since it causes more radioactive contaminations.

The shielding structure has been designed to guarantee a large sample space, low background and easy operation. The sample chamber is surrounded by 5 cm (15 cm for the base plate) of oxygen-free, highly pure copper made by the Chinalco Luoyang Copper Co., Ltd [50]. Three layers of ordinary lead, each 5 cm thick, surround the copper(see Fig.??(a) and (b)). The ²¹⁰Pb activity of lead is about 100 Bq/kg. All lead bricks were carefully cleaned by ethanol before installing. Outside the lead are 10 cm borated polyethylene plates to prevent penetration of ambient neutrons. The upper copper plate, closing the sample chamber, carrying the upper lead bricks and borated polyethylene plates, are placed on sliding rails in order to open or close the shield easily. The whole system is flushed by boiling nitrogen from the cooling dewar. The Monte Carlo simulation shows the internal background count rate of GeTHU within 40 keV to 2700 keV is only 0.0007 cps or so.(see Fig.8(c))

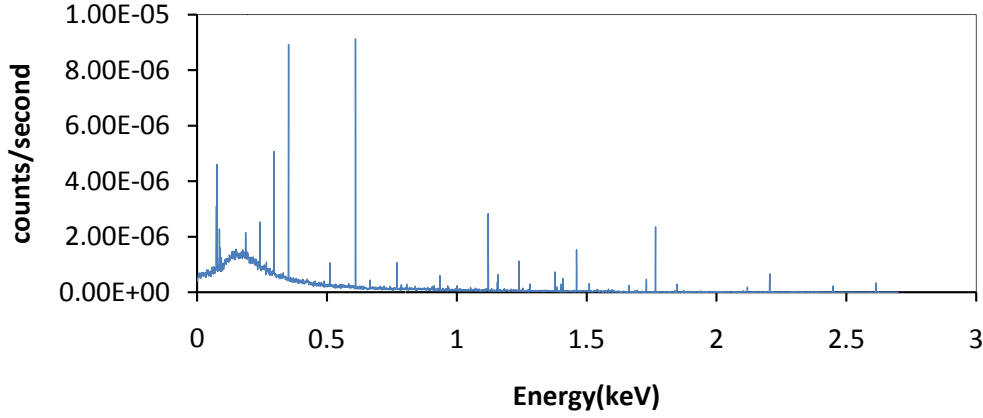
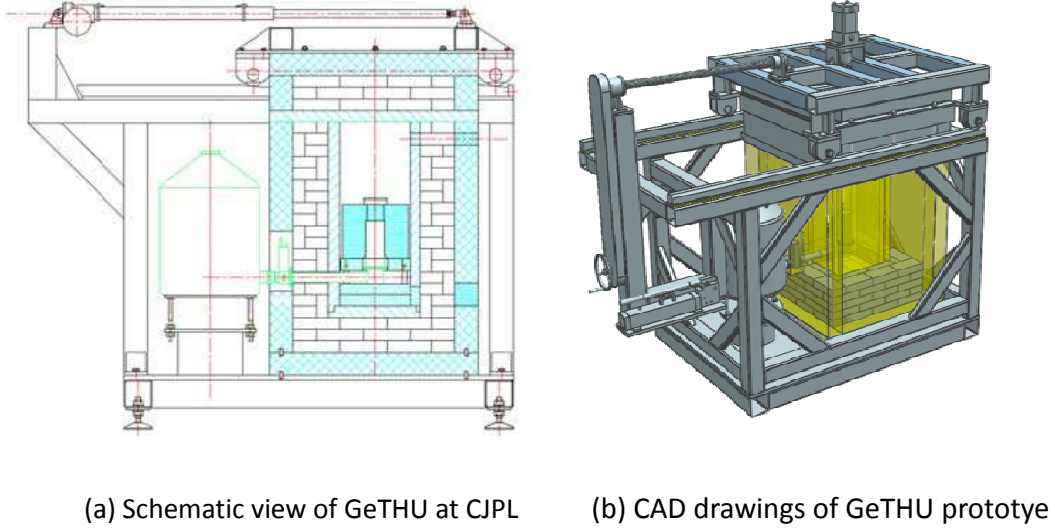
C. CJPL key performance(specification) + simulation

1. The Radioactivity of surrounding environment at CJPL

Original rock samples at different positions in the cave were collected before construction and the concrete samples were collected during the construction. All samples were measured and analyzed by low-background HPGe gamma spectrometer. The measurement results are following: the radioactivity concentrations of ²²⁶Ra, ²³²Th and ⁴⁰K of rock samples are 1.8 ± 0.2 Bq/kg, < 0.27 Bq/kg and < 1.1 Bq/kg; and that of concrete samples are 1629.3 ± 171.3 Bq/kg, 6.5 ± 0.9 Bq/kg and $19.93.4$ Bq/kg.

Beside the sample measurement, a portable gamma spectrometer manufactured by ORTECTM is used to characterize dispersed radioactive nuclides in the environment at CJPL areas. A portable HPGe spectrometer is used to measure the gamma flux at CJPL. The detector consists of a HPGe crystal with a mass of 709 g, the signals from which will be stored and analyzed by the ORTECTM DigiDART multichannel analyzer(MCA). The spectrometer is set up to measure gamma ray with energies up to 3 MeV and the energy resolution(FWHM) is 1.6 keV at 1.33MeV. Fig.9 shows the in-situ gamma spectrum in different places.

FIG. 8: The ultralow background HPGe gamma spectrometry at CJPL.



(c) The background of GeTHU with Monte Carlo simulation

2. Cosmic Ray (Muon)

The main components of cosmic ray which can pass through rock stratum of the mountain are muon and neutrino. The neutrino component can be ignored because of its small interaction cross section with the detector materials. However, it's very important to know the exact flux of cosmic-ray muons for estimating the background event rate caused by cosmic ray directly or indirectly.

In order to obtain the exact value of the muon flux in CJPL, 6 plastic scintillation detectors are employed. The volume of plastic scintillators is $1\text{m} \times 0.5\text{m} \times 0.05\text{m}$. 6 detectors are divided into groups A and B. Each group has three plastic scintillation detectors. The three plastic scintillation detectors of each group are put in erect on a shelf. The up-down distance from one detector to the neighbor one is 0.20 m. The gap between the two groups is about 0.20 m. Data are taken by a DAQ system and the LabView is shown in Fig.10.

The performance of the whole detection system was investigated on the ground nearby entrance of east end of the tunnel before measurements began inside CJPL. The triple coincidence event of the 3 plastic scintillation detectors in one group is caused by cosmic ray muons. The signal of muon event is much larger than the noise, so the experimental environment is very clean.

The preliminary result is 0.16 per square meter per day, i.e. about 1 of 10^8 muons on the ground.

FIG. 9: In-situ Gamma spectra in 3 places: CJPL Hall-green line, CJPL PE shielding house-purple line, Ground laboratory outside Jinpin Tunnel -blue line.

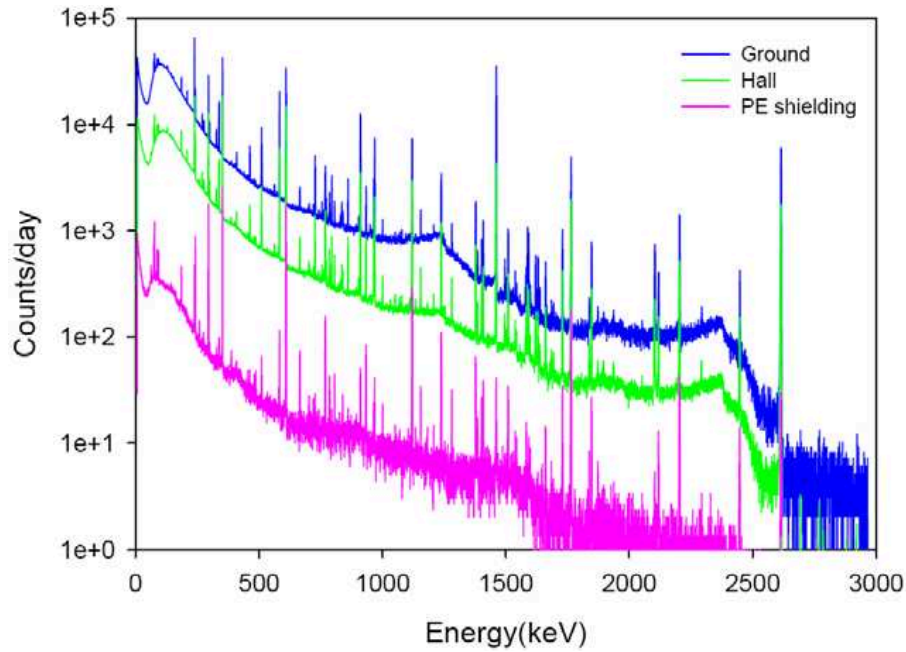
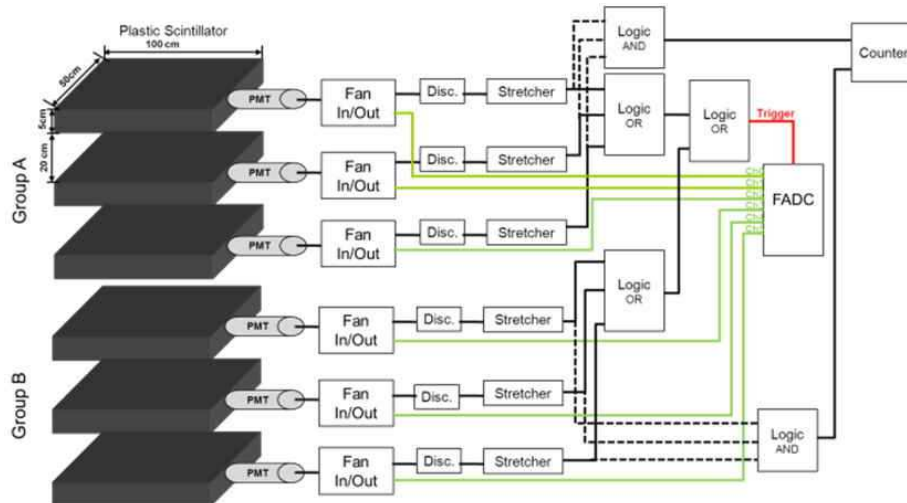


FIG. 10: Schematic diagram of cosmic ray muon detect system.



3. Radon Monitoring in CJPL

A decay product of ^{238}U , the noble gas ^{222}Rn as well as its decay daughters, also 'observably' contribute to the natural background radioactivity in underground laboratories as it is emanated from the rock and can rather easily enter the detector. Variations of the air radon concentration both in the hall and shielding house are continuously measured using two Alphaguard radon monitor manufactured by SAPHYMO GmbH (see Fig.11). During long period monitoring, the average air radon concentration is $\sim 100\text{Bq}/\text{m}^3$ without ventilation and $50\text{Bq}/\text{m}^3$ with ventilation.

FIG. 11: Radon Monitor in CJPL experiment Hall.

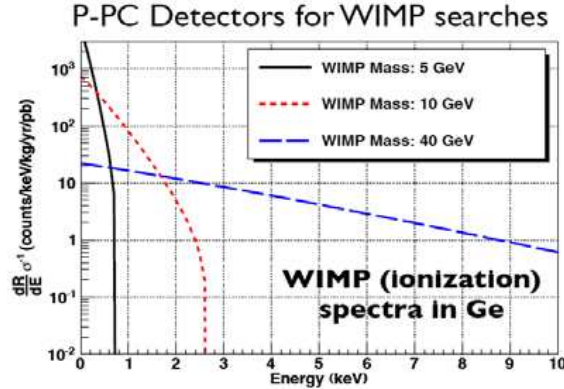


V. THE CDEX EXPERIMENT

A. Introduction to CDEX

The main physics goal of the CDEX project is to search for WIMPs in a mass range of 10 GeV with sensitivity better than 10^{-44}cm^2 . Because of much more advantages, such as low radioactivity, high energy resolution, high matter density and stability at work, the CDEX adopts the High purity point contact Germanium PCGe as the target and detector. The recoil energy of Germanium nucleus for low mass WIMPs is only several keV (Fig.12). Considering the quench factor the threshold of detection should be 100-300 eV for the WIMPs within the range less than 10 GeV. The mass target or detector should be as large as possible because of low event rates. The detector mass of the first phase CEDX-1 is 1 Kg and that of the second phase CDEX-10 is 10 kg. The final goal of the CDEX project is to set up to a ton-scale mass Ge detector CDEX-1t in the CJPL.

FIG. 12: The recoil energy of PCGe for deferent WIMP mass.



Obviously, the CDEX is a kind of ultra-low-background experiment. The biggest challenge is to reduce the background event rate to an acceptable level. The expectation of background count level is less than 0.1cpd/keV/kg. To ensure its successful operation, the CDEX must:

- hold the detector in the CJPL deep underground laboratory;
- establish an efficient shielding system to reduce the background further;
- design a large mass and low threshold detector with tiny amount of internal radioactive isotopes.

As mentioned above, the CJPL, which has an overburden of about 2400m rock, provides an ideal place to host the CDEX. In the following, we are going to briefly introduce the detector and the shielding system.

1. Detector

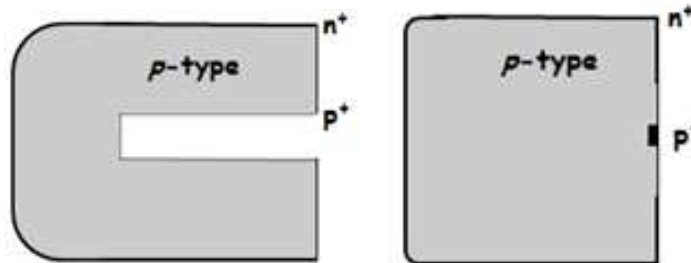
The physical aim of the CDEX composes an unprecedented challenge to the design of the CDEX detector. In summary, the detector should have the following features:

- 1 Kg to 1000 kg of detector mass to compensate the extremely low cross-section, namely substantially increase the event rate;
- 200-400 eV threshold; This is because the recoil energies are low, and furthermore only a fraction of these (a low energy quenching factor for Ge recoil of O(20)%) is generally in a detectable form, such as ionization.
- very low concentration of internal radioactive isotopes.

As a semiconductor detector made of the purest material on the earth, the HPGe detector was first proposed to detect WIMP by our group in 2004. By using arrays of commercially available HPGe diodes (5 g, 1pF capacitance), TEXONO achieved 300 eV energy threshold. But further increase of the readout channels and monetary investment prevents the detector mass to reach an O(kg) scale.

In order to compromise the mass constraint and energy resolution, small semiconductor detectors usually are the conventional HPGe coaxial detector with low noise and threshold, instead, the CDEX proposes to use a point-contact HPGe detector (herein named PCGe) to directly detect the ionization effect of the recoiled Ge nuclei. Fig.13 shows the configurations of coaxial HPGe (left) and PCGe (right) detectors. By using point contact technology, a PCGe detector can reach an order of 1 kg of mass with very small capacitance (an order of 1pF) and promising intrinsic noise characteristics. Besides the requirements on mass, energy resolution and threshold, it also has advantages that its intrinsic ability to distinguish multi-site from single-site particle interaction and surface events is remarked. The mass of the detector array can reach a scale up to O(10)kg or even O(1000)kg.

FIG. 13: The configuration of Coaxial HPGe (left) and Point-contact HPGe(right).



2. Shielding system

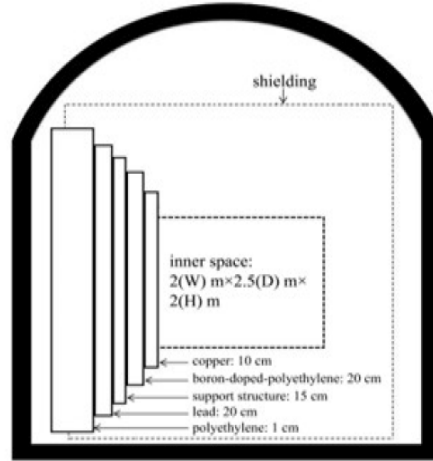
The layout of the CDEX is shown schematically in Fig.14. It is located in the CJPL, which has a PE (polyethylene) layer with a thickness of 1 m built to decelerate and absorb fast neutrons. Taking into account the commonly accepted WIMP density and elastic scattering cross sections, the expected event rate is estimated as $< 0.1\text{kg}^{-1}\text{day}^{-1}\text{keV}^{-1}$. These extremely rare events are very difficult to be distinguished from the high backgrounds which come from cosmic rays and natural radioactivity. Then the passive and active shielding systems are proposed (shown in Fig.15). The outermost layer is a 20 cm lead layer to reduce the environmental gamma ray radiation. The next layer is a 15 cm steel supporting structure. Then, a 20 cm PE(B) (Boron-doped polyethylene) layer is used to absorb thermal neutrons. The innermost layer is 10 cm OFHC (oxygen-free highly-conductive copper) for absorbing residual rays. The space inside the copper layer is the room for the HPGe detector and the active shielding system. To reduce the background of radon gas, the inner space of the shielding should be refreshed continuously with highly pure nitrogen gas.

Based on our Monte-Carlo simulation of environmental radioactivity and cosmic-ray using Geant4 Monte Carlo codes, the environment of the CJPL (rocks and concrete): neutrons yielded from the rock and reaching the innermost region of the passive shielding system is $3.129 \times 10^{-12}\text{cpd}$, the neutrons yielded from the concrete layer and reaching the innermost region of the passive shielding is $6.490 \times 10^{-10}\text{cpd}$, these two quantities are much smaller than the criteria for neutron background demanded by our expected goal. For the passive shielding system itself: we mainly consider the neutron background yielded from the lead and copper shielding, the unit contents of ^{232}Th and ^{238}U have been simulated, the result is that the neutrons which are produced by 1ppm of ^{232}Th in lead and finally reach

FIG. 14: The layout of CDEX and surrounding rock.



FIG. 15: The schematic diagram of the proposed passive shielding system.



the innermost region of the passive neutron shielding are 3.909×10^{-5} cpd, the neutrons which are produced by 1ppm of ^{238}U and finally reach the innermost region of the passive neutron shielding are 5.848cpd. The neutrons which are produced by 1ppb of ^{232}Th in copper and finally reach the innermost region of the passive neutron shielding are 1.480×10^{-4} cpd, the neutrons which are produced by 1ppm of ^{238}U and finally reach the innermost region of the passive neutron shielding are 2.289cpd. Thus the neutron background from the environment of the CJPL could be reduced very efficiently by the shielding of the CDEX. The remaining neutron background mainly comes from the passive shielding system itself. In order to realize our expected low background, we have to restrict the radioactive content of the copper and lead bricks.

Different active shielding methods are proposed for different phases of the experiments. In the first phase, the CDEX-1, CsI(Tl) or NaI(Tl), a veto detector surrounding the HPGe detector is proposed. The Liquid Argon LAr veto is proposed in the second phase CDEX-10. In this design, the LAr detector serves as both the passive shielding detector and the low temperature media for the HPGe detector.

B. CDEX-1

As the first phase of the CDEX experiment, a detector with 1 kg mass scale of HPGe, named CDEX-1, is designed and runs first. It includes a ready-made 20g ULEGe [51] (also Ultra-LEGe, Ultra Low Energy high purity Germanium detector) detector and a 1kg-PPCGe(P-type Point Contact Germanium) detector.

1. 20g-ULEGe

The 20g ULEGe (N-type), manufactured by Canberra, France in 2005, actually consist of 4 duplicate crystal elements. Each 5g element whose cross section structure shown as Fig.16, has a semi-planar configuration with a P+ contact on the outer surface, and an N+ contact of small diameter. Other surface encircling the N+ contact is passivated to suppress the surface dark current. Fig.17 depicts the horizontal cross section of the cryostat and the positional relationship of the 4 crystals. The cryostat end cap opens a 0.6mm thick carbon composite window so that an external soft X-ray calibration can be carried out. Near the N+ contact, a low noise FET is installed which reads the signal and inputs it to a pulsed optical feedback preamplifier. Each crystal element has two identical outputs, which are connected to high impedance input of the downstream modules.

FIG. 16: 20g-ULEGe detector geometry.

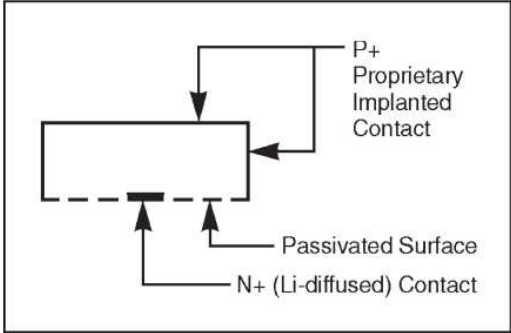


FIG. 17: The horizontal cross section of cryostat and crystal array.

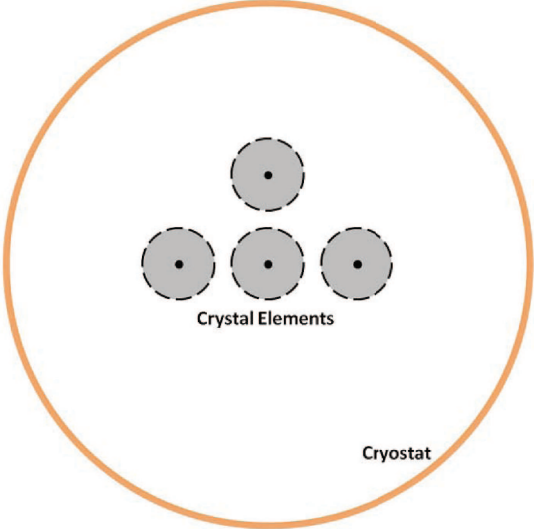
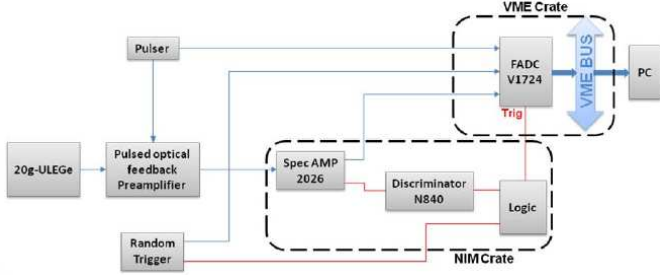


Fig.18 simply describes the DAQ setup of the 20g-ULEGe experiment. The output from the preamplifier is directly connected to the conventional spectroscopy amplifier (Canberra 2026), which has high input impedance. The signal is then split: one is input into a FADC (CAEN V1724, 100MHz bandwidth) while the other is input into a discriminator to generate trigger control. Meanwhile, random trigger and pulse modules are used to study efficiency feature etc. The data from the FADC is transferred to PC through a duplex optical fiber.

2. 1kg-PPCGe

The Germanium detector 1kg-PPCGe(P-type) manufactured by Canberra, France, was transported to the CJPL in 2011. This 1kg-PPCGe detector, using new point contact technology, has a larger mass: 1kg (single crystal). The

FIG. 18: Simplified Schematic Diagram of 20g-ULEGe DAQ setup.



crystal cylinder has an N+ contact on the outer surface, and a tiny P+ contact stands as the central electrode. The diameter and depth of the P+ contact are in order of 1 mm. The small diameter reduces the capacitance (order of 1pF) of the detector, and readily improves the intrinsic noise standard [52, 53]. The cryostat is designed fully-closed within 1.5 mm thick copper layer, and there is no thin polymer film window.

The 1kg-PPCGe possesses two preamplifiers, as shown in Fig.19. The p-type contact signal is read out by a pulsed optical feedback preamplifier, with a low noise EurIFET nearby, while the n-type contact signal is read out by a resistive feedback preamplifier. Both preamplifiers have two identical outputs: OUT T and OUT E. All outputs are connected to the downstream modules which have high input impedance.

For the second phase of CDEX-1 experiment, the DAQ set up for running the 1kg-PPCGe is simply illustrated in Fig.20. Considering the low energy range we are interested in, a fast timing amplifier (Canberra 2111) is utilized to amplify the preamplifier signal, and then input into a faster FADC (CAEN V1721, 500MHz bandwidth). The other preamplifier outputs are directly connected into conventional spectroscopy amplifiers (Canberra 2026). The signal from N-type contact is then fed into the FADC (CAEN V1724, 100MHz bandwidth); while the one from P-type contact is split into the same FADC and a discriminator for trigger control respectively. Again, the random trigger and pulse modules are used to study efficiency features and etc. The data are transferred into PC's through a duplex optical fiber.

FIG. 19: The front-end electronics of 1kg-PPCGe in CDEX-1.

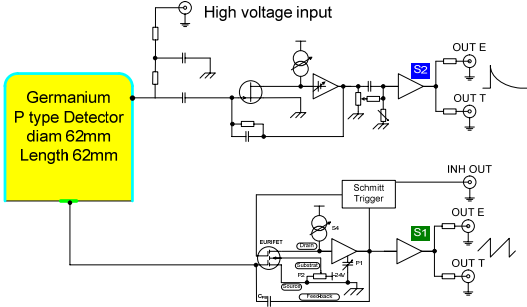
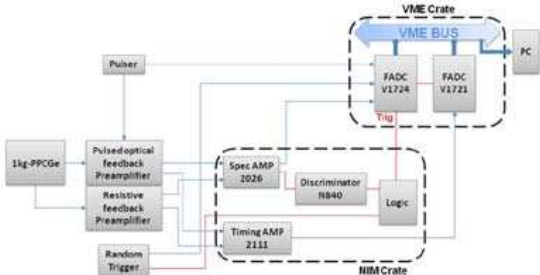


FIG. 20: Simplified Schematic Diagram of 1kg-PPCGe DAQ setup.



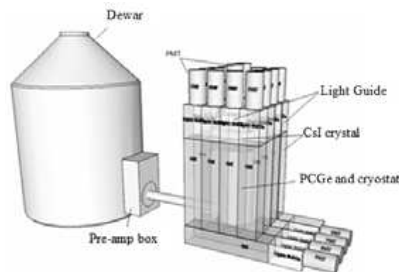
3. Veto detector

The passive shielding system has been well established which can efficiently block the outside gamma ray coming inside, but cannot be 100%. Besides, the shielding materials, even the HPGe detectors, have radioactivity themselves at certain levels. If these rays deposit energy in the HPGe detector, it would be hard to be distinguished from the WIMP signals. Luckily, due to the extremely low cross section of WIMPs colliding with ordinary matter, it is almost impossible that WIMPs can deposit energy both in the HPGe detectors and surrounding materials at the same time. So, the Veto detectors are installed to surround the HPGe detector. By that design, the output signal from HPGe is used as the trigger signal, if there is also signal from surrounding Veto detectors during the same time window, the detected event is not from collisions between WIMPs and detector material and will be filtered. In addition, these Veto detectors are also used for passive shielding. In summary, the Veto detector should have following features:

- High Z and high density to achieve high veto efficiency and the high shielding ability;
- Low internal radioactivity;
- Low threshold to increase the veto efficiency.

In CDEX-1, CsI(Tl) or NaI(Tl) scintillation detectors are proposed for the Veto detector. Except the features mentioned above, the CsI(Tl) or NaI(Tl) scintillation detectors have capacity of carrying the pulse shape discrimination (PSD), robust (reasonably soft and malleable, less brittle and deliquescent for CsI(Tl)) and easy to make a large volume. Fig.21 shows the 18 CsI(Tl) crystal array of veto detectors arranged around the cryostat, and each one is read out by a PMT through a light guide. The advantages of this design are: 1) the transportation length of scintillation light is short, good for light collection and lowers the threshold; 2) easy for extension to accommodate larger PCGe detector; 3) the CsI(Tl) crystal bar is easy to produce.

FIG. 21: The schematic diagram of CsI(Tl) veto detector system.



C. CDEX-10

Two detectors of CDEX-1, the 20g ULE-HPGe and 1kg-PPCGe, are running at present in CJPL. The data analysis framework has also been set up for the forthcoming data analysis. The CDEX-1 experiment is just the first stage for using low energy threshold Ge detector to directly detect dark matter. The CDEX-1 experiment will provide more detailed information about the Ge detector performance and the background in the active and passive shielding systems of the CDEX in CJPL; at the same time, the preliminary physical results on dark matter search with these two Ge detectors will be given by the CDEX Collaboration soon.

According to the recent model-dependent estimation on the cross sections of collision between WIMPs and nuclei, the detector target mass should be up to ton-scale if the dark matter experiment tries to "see" the dark matter, i.e. achieve statistically sufficient event rates with relatively high sensitivity. So the CDEX collaboration plans to directly detect dark matter with low energy threshold Ge detector of ton-scale target mass. There are several basic conditions which should be considered for the future ton-scale Ge detector. First, the Ge detector module with low energy threshold down to sub-keV scale and enhancing the target mass of the total Ge detector can be realized by increasing the number of the Ge detector modules. The second one is that the Ge detector has to include a cooling system to guarantee a low working temperature for the Ge detector. The third one is that the Ge detector should possess a veto detector serving as an active shielding against the background contribution coming from the Ge detector itself and the material near the Ge detector.

With this consideration, the whole detector system is composed of two parts: the Ge detector which can be up to ton-scale, is equipped with 1kg mass Point-Contact Ge detector modules; another part is the Liquid Argon veto detector serving as the cooling system and active shielding. In order to test the conceptual design of this detector and learn more details about the technology and gain experience on the Ge detector and LAr veto system, the CDEX Collaboration has designed and will run a 10kg-scale Ge detector with LAr cooling and veto system firstly.

Based on the studies of the PCGe detector, a new idea about the active shielding system of the PCGe has emerged. The PCGe detector will reach a ton-scale in the future in order to be more sensitive to dark matter detection. In that scenario, the active shielding system with the solid scintillators would be very difficult to enclose the larger PCGe array system, while keeping the PCGe detector to be cooled down to the liquid nitrogen temperature. So a new type of active shielding technology for large-mass array PCGe system has to be invented. The Liquid Argon (LAr) is a good candidate. The temperature of LAr is suitable for the Ge detector and LAr is also a kind of scintillator and can serve as an active shielding system while the Ge detector is immersed into it.

The CDEX Collaboration has completed the physical and structure simulation study on the CDEX-10 detector system, and also the conceptual design and related studies on the Ge detector, LAr veto detector, LAr cooling system and passive shielding system.

The structure of the whole CDEX-10 detector and the shielding system are shown as follows. The interior of a 1 m thick (red) polyethylene serves as a neutron shielding room. This neutron shielding room had been constructed as the CJPL was under construction and now we have started to carry out several experiments inside this polyethylene room. The blue layer is lead shielding against the outside gamma background. The yellow layer is Oxygen Free High purity Copper (OFHC) which shields out the residual gamma background passing through the lead layer and also shields the internal background radiated by the lead shielding. Inside the OFHC layer there is the LAr veto detector system which serves as both active and passive shielding. Three 0.5 Kg or 1 kg PCGe detectors are encapsulated into ultra-pure copper or aluminum tubes which are highly evacuated. One block of the OFHC (Blue box) is mounted to shield the PCGe detector from noise produced by the electronics in the tube. Several encapsulated tubes with three PCGe detectors are immersed in the LAr vessel for cooling and active shielding. The Total mass of the PCGe detector is about 10 Kg. Part of the energy is deposited and the scintillation light is produced when gamma or beta ray enters the LAr. The scintillation light is read out by the photomultiplier tubesPMTand then the signal can serve as a veto signal.

The Ge detector tubes on the 1 kg p-type point-contact Germanium detector has been manufactured by the Caberra Company according on the CDEX requirement and design. The 1 kg p-type PCGe detector for dark matter search experiment is also the biggest one in the world till now. The 1 Kg-PCGe detector has been taking data after its performance test.

In this CDEX-10 detector, the scintillation light is read out by the PMT on the top of the LAr volume. The number of PMT is determined by the detail of the physical design and the following plot gives the layout plot of the PMT deployment.

The design of the cooling and active shielding systems for CDEX-10 LAr has been completed. From the physical point of view, the main requirements for the LAr cooling and active shielding systems are to keep the LAr temperature uniform and stable within a small temperature region to alleviate the temperature dependence of the performances of the PCGe detector, and to prevent formation of gas bubble and concomitant tiny vibration of LAr which may induce extra noise in the Ge detector. A number of methods for satisfying such stringent restrictions are considered to maintain constant liquid level and control the generation of gas bubble in liquid argon under zero boil-off conditions for long periods of time. Large convective motions and pool-boiling are avoided by thermally optimized cryogenic systems to reduce environmental heat leaks to the low-temperature cryogen, especially, an actively-cooled LAr shield that surrounds the cryostat is used against heat radiation.

D. Electronics (FADC, DAQ)

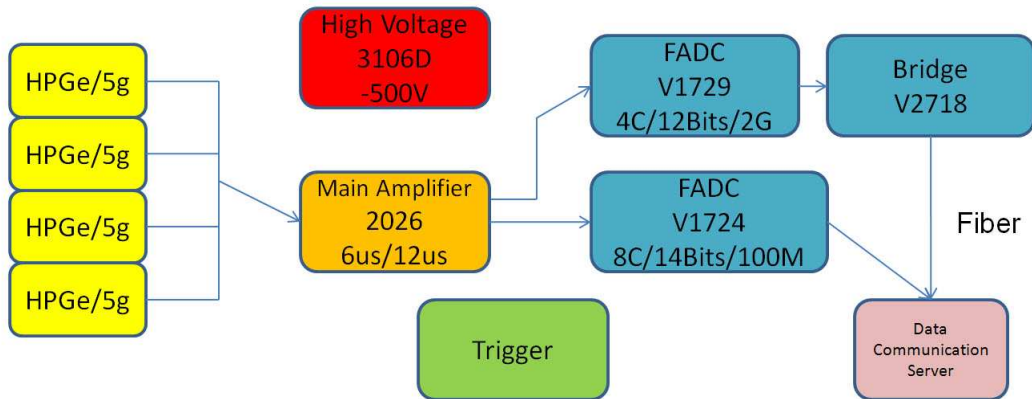
The CDEX electronics includes three parts: Electronic, Trigger System and Data Acquisition System where:

- The electronics includes the front-end amplifier, the main amplifier, the flash analog/digital converter, as well as HV power supply and the slow-control electronics etc.
- The trigger system contains the trigger system and the clock distribution system.
- The data acquisition system contains the data read-out electronics, the slow-control electronics and related data server and memory, communication, display and HMI etc.

1. The Current Design of Electronics

Considering the future development, a set of multiple-channel electronics for the CDEX detectors has been designed. Fig.22 shows the design architecture of the electronics for our CDEX. The mode is prevailing for both electronics and other parts. So, in the following discussion, a thorough description about the ongoing electronics is made first, and then we will go on describing the next generation of electronics which is under research & development, as well as the concerned engineering problems.

FIG. 22: The ongoing design architecture of electronics: CDEX.



2. The CDEX-1 and CDEX-10 Electronics Architectures

It is forecasted that the signal-readout channels of the larger-scale CDEX detector will be 100~1000 in the future. It is necessary to research and develop an electronic system which will be used for both HPGe and veto detectors. The whole electronic system includes the front-end amplifier, main amplifier, FADC and data readout etc. Now the electronic group is focusing their efforts on the design and plan of each parts of the electronic system as described in the following.

- FADC:

According to the physical demand, there are two different kinds of the FADC (Flash Analog to Digital Converter) electronics needed for reading out the pulse shape from the HPGe detector or Veto detector: one is 100MHz, 14 Bits, 16-channel FADC/GE electronic plug-in with standard dimensions of VME plugin; another is 1GHz, 12Bits, 4-channel FADC/AC electronic plug-in with standard dimensions of VME plug-in. The FADC/GE electronic plug-in is used to read out data on the slow-shaping-time signal of the HPGe, and FADC/AC electronic plug-in is used to read out the fast-shaping-time signal from either HPGe or photomultiplier tube (PMT) of the veto detector.

For convenience and to satisfy different physical demands, the design of the FADC system adopts a new concept which is also being applied in many labs of CERN. The structure uses the same VME board (Main Board) and different FADC. The experiments facilities are realized by using different FADC Mezzanine Cards. Different FADC mezzanine cards are made of FADC chips with different performance indexes and numbers, the channels are connected to the board via the high-speed plug-in. Then the same board is used to conduct data cache, processing and triggering judgment, and then the signals are read out via the standard VME bus of the front-end fiber-optic interface of the back board.

- The Readout Electronics:

The CDEX electronic readout system is integrated on the Wukong board which is an electronic product developed by the researchers of Tsinghua University, and the module RAIN200A is used to read out the data of each Wukong Board. The module RAIN200A is based on PowerPC predecessor, where Linux2.6.X is running to realize the readout data from FADC to Ethernet, with a bandwidth at least 95Mbps.

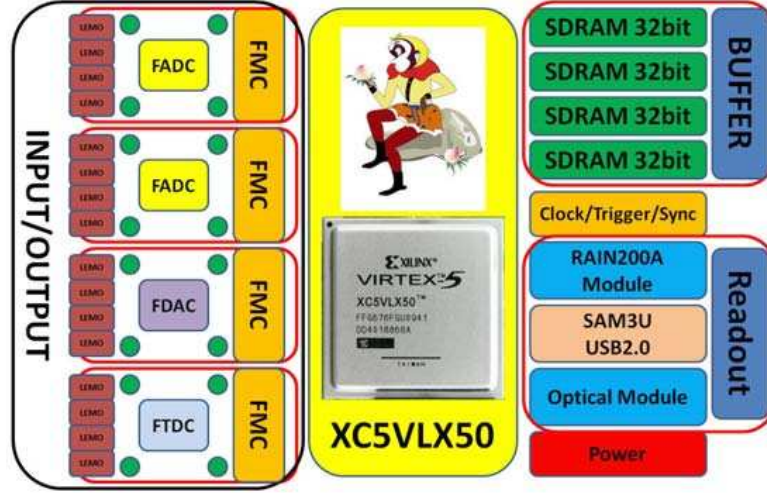
The RAIN200A has the following characteristics: The core predecessor is the 32-bit car-grade MPC5125 made by Free scale, with frequency of 400MHz; the core board is installed with a 256MB DDR2 industrial-grade memory and 4GB NAND Flash; the core board is supplied with 100Mbps Ethernet interface and USB 2.0 High-Speed interface; the system runs Linux 2.6.29 kernel with RT patch.

- DAQ:

The CDEX DAQ includes the electronic part acquiring data from the electronic units, the online data judgment, display and memory as well as the off-line data analysis etc.

Because the electronic unit uses the Ethernet and TCP/IP as the interface of data readout, DAQ needs merely to acquire data per the standard protocol TCP/IP from the electronic unit, so that our scheme is very convenient. The architecture of the entire DAQ system is also an Ethernet-based exchange one and so the standard commercial switches, routers and Ethernet cards can be used to acquire data for the DAQ. Fig.23 gives the Wukong FADC/DAQ system for the CDEX-1 and CDEX-10.

FIG. 23: The Wukong FADC/DAQ system for CDEX-1 and CDEX-10.



VI. DETECTOR PERFORMANCE

A. Physical requirement

As a detector used for dark matter detection, the most important requirement for it is its low background level. The CDEX is to detect WIMPs with a high purity germanium detector, especially focusing on WIMPs of low masses ($<10\text{GeV}$). This imposes another important requirement of energy threshold to the detector. The CDEX Collaboration adopts the Point-Contact germanium detectors (PCGe) for the low mass WIMP search which can realize a sub-keV energy threshold with kg-size mass. The ton-scale detector system of the CDEX in the future will be realized based on this kind of kg-size PCGe detector. The PCGe detector has been developed from the conventional Ultra Low Energy Threshold germanium detector. Many efforts have been contributed to optimize the application of the PCGe in dark matter searches.

- Pulse shape analysis of near noise-edge events extends the physics scope
the PCGe detector can provide ultra-low energy threshold down to less than 500eV. According to the theories on dark matter, the differential event rate of observing the recoiled nucleus scattered off by incident WIMPs exponentially increases with the decrease of its energy. So the pulse shape analysis of near noise-edge events is a very important task for the CDEX experiment to get lower energy threshold of the PCGe detector.
- Pulse shape analysis of surface versus bulk events to characterize an important background channel
The location of an event where it is detected is another important parameter for background discrimination. For a p-type PCGe detector, due to the outside N+ or P+ conjunction, there exists a thin layer which is called the "dead" layer. In fact, the thin layer is not really "dead", the events emerging in this thin layer can also give

a different pulse shape from those bulk events which are produced in the interior part of the PCGe detector. So the pulse shape discrimination methods should be developed for distinguishing the surface events from the bulk events.

- Sub-keV background clarification and suppression

For the PCGe detector with a sub-keV energy threshold, it provides us a new energy window where so far no researches have ever covered this energy region due to relatively high energy threshold of those detectors. The CDEX experiment should first clarify the source and types of the background in the sub-keV energy region. Based on the present knowledge, a method for the background discrimination and suppression will be developed.

- Fabrication of advanced electronics for Ge detectors

The pulse shape discrimination methods have been developed for suppressing noise, especially near the energy threshold, and discrimination of the surface events from bulk events. All these methods to obtain lower energy threshold and low background level are based on the performance of the front-end electronics of the PCGe detector. So another important requirement to the PCGe detector is the fabrication of advanced electronics for Ge detector which provides relatively low noise level.

B. Performance of CDEX-1

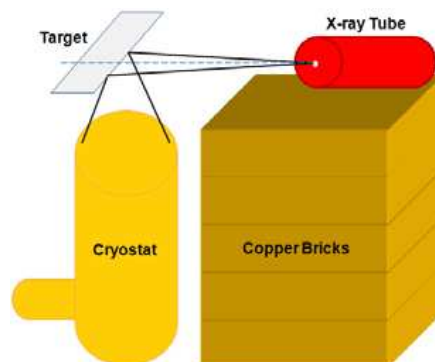
Since our first testing run of 20g-ULEGe in November of 2010, we have obtained some data during both commissioning period and formal data taking period. Data analysis is being undertaken for determining the final spectra, and the properties of the 20g-ULEGe in this new CJPL environment have been known.

The Commissioning period data of 1kg-PPCGe have also been acquired. The properties of this detector are shown in the following subsections.

1. Linearity calibration of the detector 20g-ULEGe and 1kg-PPCGe

Because of its small volume, the detection efficiency of 20g-ULEGe is relatively low to get prominent peaks for calibration, even though the calibration period was prolonged to several months. Withal, there is no source available for further test in the CJPL at present. An X-ray tube [54], which can generate X-ray of up to about 30 keV, is applied as a substitution of the source. When the X-ray generated by the tube hits the mixed powders of titanium dioxide (TiO₂) and potassium permanganate (KMnO₄) the characteristic X-rays can be used for the high gain (low energy range) calibration. The surrounding copper shielding contributes characteristic X-rays as well. Thanks to the thin carbon composite window of 0.6mm, overwhelming amount of the low energy X-rays are able to penetrate and deposit energies in the crystals. Sketch of the calibration for the 20g-ULEGe is illustrated in Fig.24.

FIG. 24: Sketch of calibration for 20g-ULEGe by X-ray tube.



The calibration result of the 20g-ULEGe are shown in Fig.25, with each sub-figure in accord with a 5 g sub-detector. In this scheme, characteristic X-rays of titanium, manganese and copper, coupled with random trigger [55] (zero point) are used (Table.I). From the fitting results of the seven points, we can observe a good linearity in the low energy range below 10 keV. Moreover, the region above 10 keV can be studied with available radiation sources.

FIG. 25: Calibration result of 20g-ULEGe.

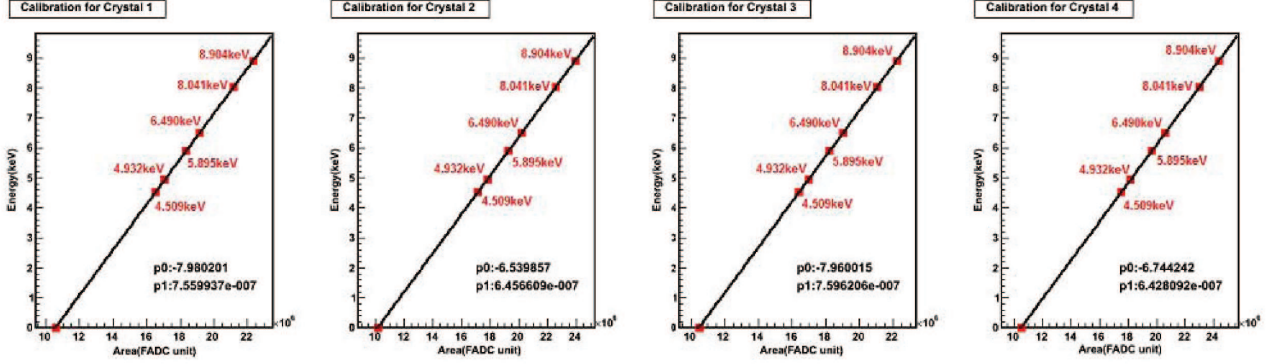
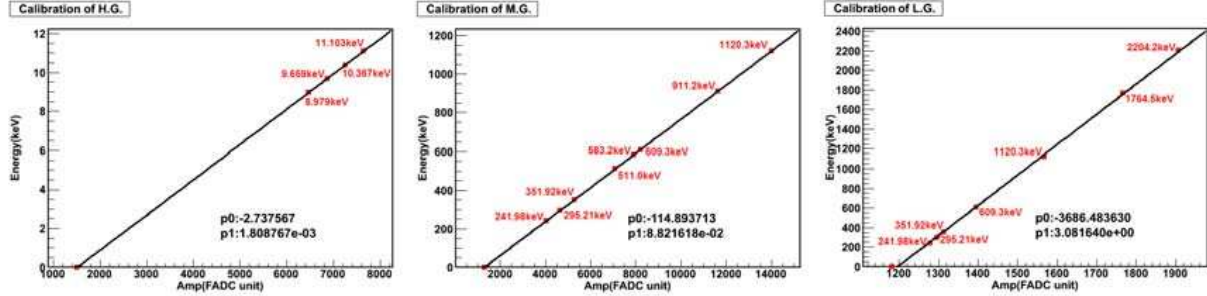


TABLE I: Sources for calibration of 20g-ULEGe

Source	Random trigger	Ti	Mn	Cu			
Energy (keV)	0	4.509	4.932	5.895	6.490	8.041	8.904

The 1kg-PPCGe does not have a carbon composite window, but a large volume and mass. So its detection efficiency is high enough to carry out a calibration with a few days' background data. The result of one data set is shown in Fig.26, with 3 sub-figures corresponding to different gains. The period is 21.9 days and lots of background peaks are visible. Besides the zero point by random trigger, we respectively use 4-8 points to complete the calibration fitting for different gains (Table.II). The results also display a good linearity of the 1kg-PPCGe.

FIG. 26: Calibration result of 1kg-PPCGe. Left: High Gain. Middle: Mediate Gain. Right: Low Gain.



2. Energy resolution of detectors 20g-ULEGe and 1kg-PPCGe

With the calibration data, the energy spectra as well as the properties of energy resolution have been obtained.

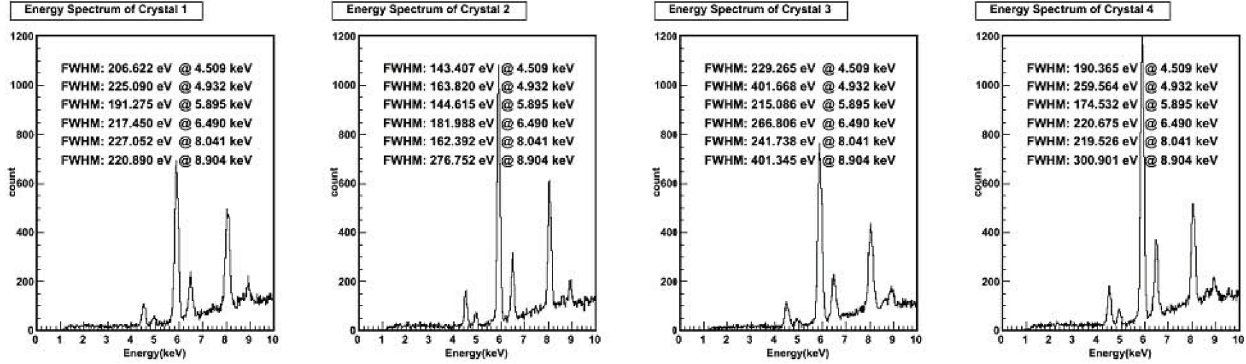
The calibrated spectra of the 20g-ULEGe are plotted in Fig.27. FWHMs (Full Width at Half Maximum, fitted to a Gaussian function) are about 200 eV at 5 keV and about 300 eV at 9 keV. The 4 sub-detectors are very close to each other in all technical indices and practical performance. Besides the statistical limit, the X-ray tube which has a wide emission solid angel and notable energy dispersion, also degenerate the FWHM. So the energy resolution of the system is expected to be better than the predecessor products.

The calibrated spectra of 1kg-PPCGe are plotted in Fig.28. The FWHMs are about 200 eV at 10.367 keV and about 3.525 keV at 1120.3 keV. For many other peaks, FWHMs are limited by statistical errors, thus need to be improved with more data accumulation.

TABLE II: Sources for calibration of 1kg-PPCGe

High Gain		Mediate Gain		Low Gain	
Source	Energy (keV)	Source	Energy (keV)	Source	Energy (keV)
^{65}Zn	8.979	^{214}Pb	214.98	^{214}Pb	214.98
^{68}Ga	9.659	^{214}Pb	295.21	^{214}Pb	295.21
^{68}Ge	10.367	^{214}Pb	351.92	^{214}Pb	351.92
$^{73,74}\text{As}$	11.103	Ann	511.0	^{214}Bi	609.3
—	-	^{208}Tl	583.2	^{214}Bi	1120.3
—	-	^{214}Bi	609.3	^{214}Bi	1764.5
—	-	^{228}Ac	911.2	^{214}Bi	2204.2
—	-	^{214}Bi	1120.3	-	-

FIG. 27: Calibrated energy spectra of 20g-ULEGe.



3. Noise level of detector 20g-ULEGe and 1kg-PPCGe

Electronic noise would crucially affect the detection threshold. To study the noise level, events by random trigger tag are selected and projected to energy spectra, which are then fitted with the Gaussian function. The FWHMs of the distributions render less than 100 eV of both 20g-ULEGe (crystal 2) and 1kg-PPCGe, which sustain the threshold lower than 500 eV. (Fig.29,30)

4. Stability of the detector

The validity of data which depict the system stability needs to be checked before overall data analysis. Several parameters describing the system behaviors are tracked over time, including triggering rate, pedestal of pulse shape, noise level, et. al.. Figs.31,32 present the triggering rate status of 20g-ULEGe and 1kg-PPCGe, in which an average rate per hour is counted. Immoderate parts, especially an anomalous discrepancy deviating from the average level, should be carefully inspected and discarded if they are proved to be invalid.

5. Trigger efficiency

Trigger efficiency is to be checked before data analysis is carried on [51]. It determines the survival fractions of the events which pass the discriminator threshold. Specific pulse generator which can supply small signal ranged at 0-2 keV can be used to estimate the trigger efficiency at lower energy regions. Such a kind of pulse generators is under development right now, and the relevant test will be held soon.

FIG. 28: Calibrated energy spectra of 1kg-PPCGe. Left: High Gain. Middle: Mediate Gain. Right: Low Gain.

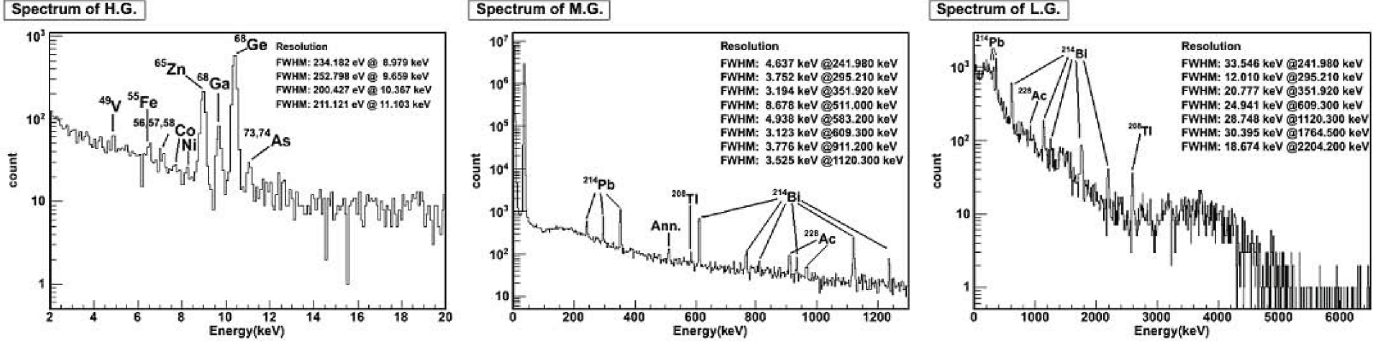
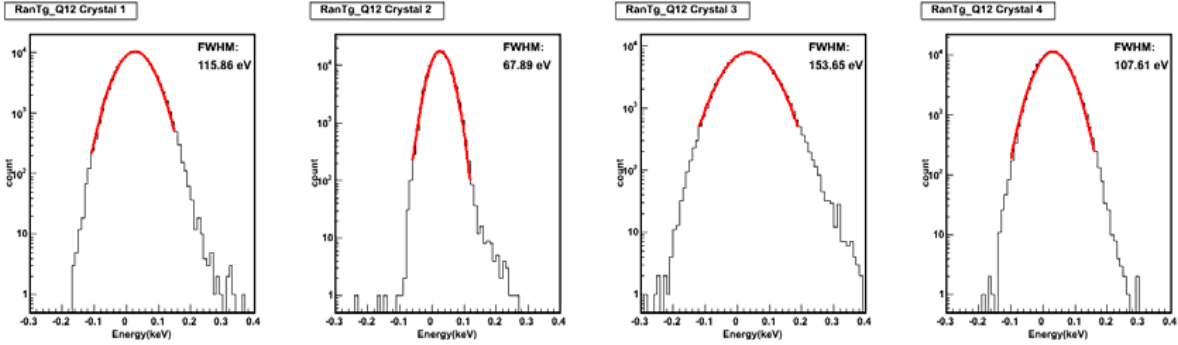


FIG. 29: Noise distribution of 20g-ULEGe by random trigger.



VII. DATA ANALYSIS

A. Process

The data analysis is a very important step to understand the energy spectra of the HPGe detectors. Usually there are three sources contributing to the HPGe spectra: electronic noises and microphonic interference, physical background events as well as dark matter events. The purpose of the data analysis is first to discriminate out the noise, physical background events from the total energy spectra. Different methods need to be developed according to the characteristics of different sources.

The signal shape of electronic noise and microphonic interference are not in the Gaussian-like wave form in which the physical events should be, then can be distinguished through some PSD (Pulse Shape Discrimination) method. Various parameters, time-to-peak, rise time and fall time, for instance, describing wave form of the signal can be designed and used for differentiating in parameter plots. In contrast to the anomalous wave form, analog to the Gaussian-like pulse shape would be a criterion for identifying the type of the sources in the calibration data.

In particular, electronic noise exerts a crucial impact on the threshold and needs to be handled with great caution. Physical events, in principle, follow the Gaussian distribution in 2-D energy-energy parameter plot. So the threshold can be lowered in this parameter plot than in a single energy spectrum plot. A noise edge cut, which exists along the tangent of the Gaussian distribution, is then set to lower the threshold. Since the cut is related to energy, the efficiency-energy curve should be estimated by the pulse calibration data or anti-Compton tagged data.

Usually in experiments of searching for dark matter one observes recoiled nuclei, such events might be tangled with the physical background caused by neutrons and electron recoil events. Several experiments, such as CDMS[56], XENON100[57], CRESST-II[58] et. al., use two distinct signals such as scintillation and ionization to reject the electron recoil events simultaneously. But it's not the case in the CDEX. The CDEX only measures the energy deposit of ionization. Another difference is that the CDEX needs to consider the quenching factor of energy deposit for the recoiled nucleus.

As the pulses caused by the electron recoil and nucleus recoil do not appear different, the normal PSD method would be less efficient here, some other aspects need to be viewed. There are mainly two ways to subtract the background

FIG. 30: Noise distribution of 1kg-ULEGe by random trigger (High Gain).

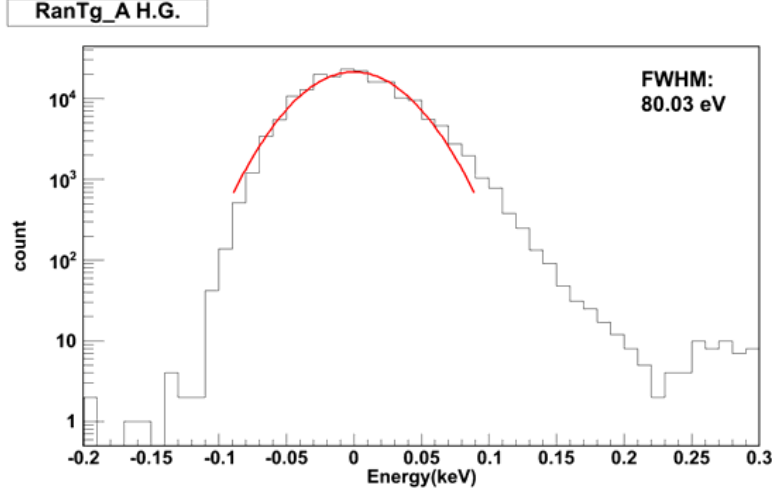
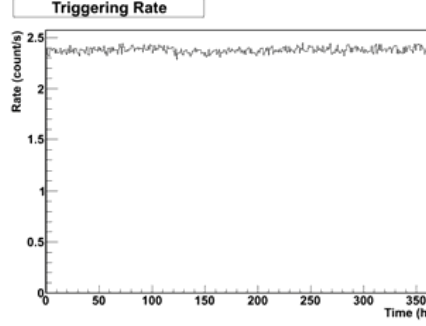


FIG. 31: Triggering rate status of 20g-ULEGe.



events. One is to statistically eliminate the visible and invisible characteristic x-ray peaks; while the other is to apply some algorithm to reduce surface events occurring in the thin insensitive layer. In the low energy region which we are interested in, visible characteristic peaks usually come from the K-shell X-rays and the invisible ones are caused by the L-shell X-rays' contribution, both of them have been analyzed theoretically and experimentally in some details[59]. On the other hand, the surface insensitive layer of the PPCGe detector has a weaker electric field therefore can cause distortion of energy deposition. Such a kind of events would have slow pulse shape from preamplifier, but is degenerate with the electronic noise. The Wavelet method [60] can reduce noise by filtering and shaping the signal sample.

With all the aforementioned processes, the final energy spectrum is obtained. Based on selected physics and statistical method, the final spectrum is then interpreted into physics result, namely the common exclusion curves.

B. Strategy

In order to measure the cross sections for low WIMP masses, elaborate data analysis is essential to lower the threshold and single out background events from raw data. The threshold can be lowered by getting rid of noise events, and the non-WIMP event rate can be suppressed by deducting the microphonic events as well as physically identified non-WIMP events. Microphonic events, coming from violent changes of environment or instability of the system, usually have abnormal pulse shape. Non-WIMP events may consist of multi-site events (events with several incident particles coincidentally), surface events (events with energy deposited in the dead layer of the surface), et. al.. To attain this goal, some variables or parameters are defined, either event by event or statistically. Fig.33 illustrates the notation of several empirical main parameters. Ped, e.g., is calculated as the average pedestal within the first 200 FADC time units.

Some basic cuts for selection of pulse shapes, such as the stability of pedestal, time-to-peak, as well as linearity

FIG. 32: Triggering rate status of 1kg-PPCGe.

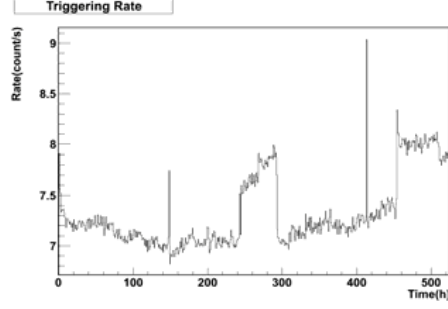
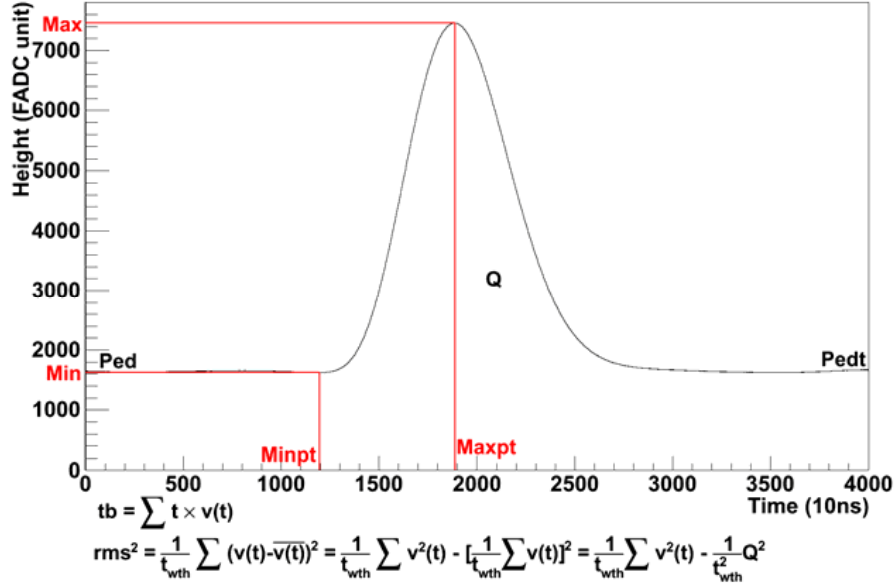


FIG. 33: Notation of several parameters.



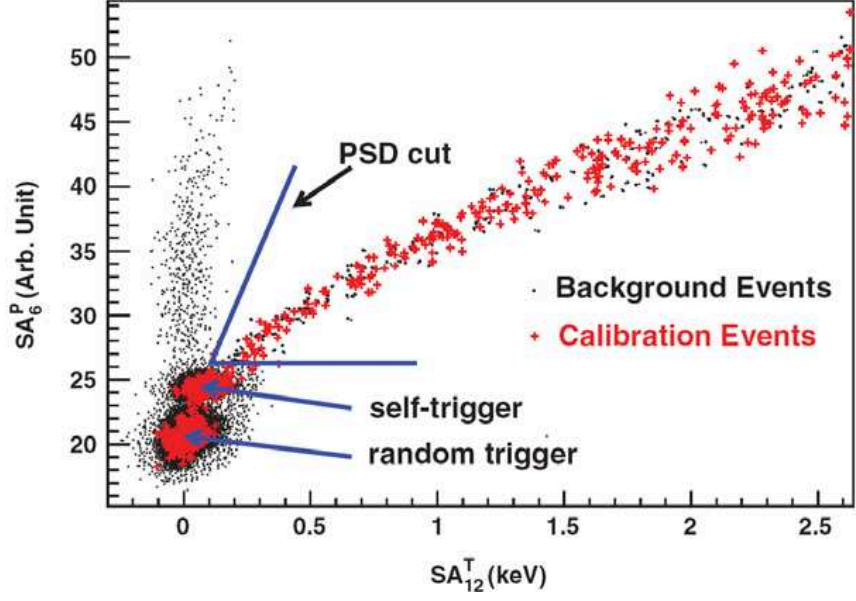
between area and amplitude, are applied firstly. After the pulse shape selection, three different crucial cuts are utilized as described in the following subsections. Then the derived final spectrum is used to interpret the physics, commonly as making exclusion plots or indicating islands in the parameter space.

Moreover, to identify the noise and microphonic events, reference pulse shape of physics events are needed. Such physics events can be selected within peaks of characteristic x-ray, either from calibration data or from background measurement.

1. PSD cut

Noise and microphonic events having different pulse shapes from the physics events, can be distinguished through the PSD (Pulse Shape Discrimination) method. The parameters for each event pulse with different shaping time are then considered, and the scattered plot is shown in Fig.34. The two parameters are the pulse amplitude with shaping times of $6\mu s$ and $12\mu s$ respectively. Red dots roughly along the diagonal stand for the physics and noise events, while the black dots in the band near the axes correspond to the interference events. So taking the straight lines (blue-colored) as cuts, we are able to discard the microphonic events.

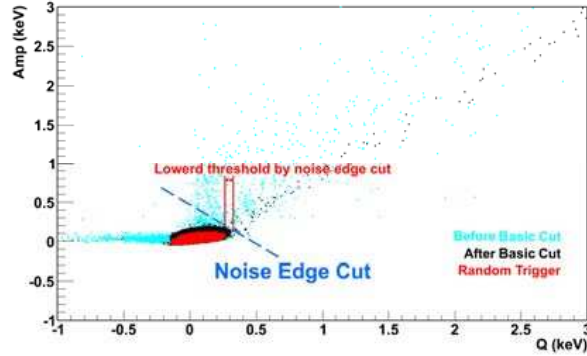
FIG. 34: Illustration of PSD cut [51].



2. Noise edge cut

In principle, the pulse amplitude distribution of the noise events is Gaussian. So in the 2D (pulse amplitude and pulse area) parameter plot, the distribution seems like an ellipse (Fig.35). Whenever they are projected to either axis, the bulge would degrade the noise level. Noise edge cut is then used to reduce the noise events and hence lower the threshold. The key point is that since this cut is related to the energy, the efficiency curve has to be applied to make corrections.

FIG. 35: Illustration of noise edge cut.

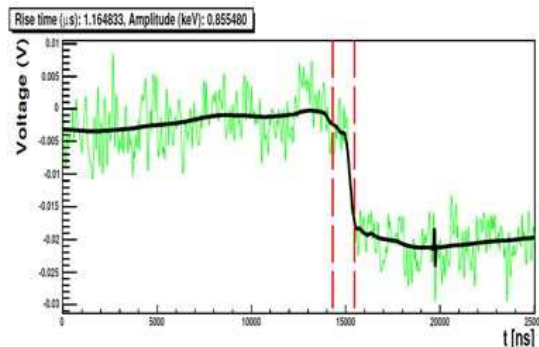


3. Surface event cut

Due to the manufacturing limitation, the N+-type surface layer of the PPCGe is thick, in which the electric field is weaker than in the crystal bulk so that the energy deposited in this layer cannot be efficiently collected. This layer is then named as the dead layer or insensitive layer, and the recorded events with energy deposited in this layer are called as surface events. The surface events have a longer charge-collection time and slower pulse shape, which may be picked out by the time parameter cut. The rising time of the fast pulse at the preamplifier is chosen as the time parameter. However, in the low energy range which we are highly interested in, the signal-to-noise ratio becomes not high enough to finely deduce the parameter. Green curve in Fig.36 shows a raw fast pulse. Marino [60] suggested a

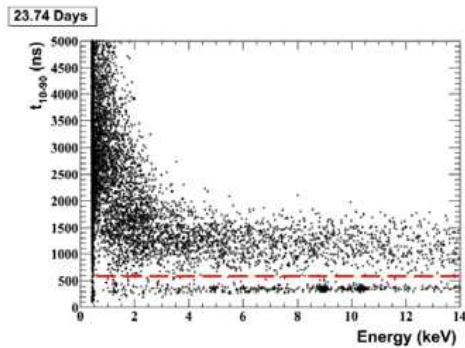
method that one can use a wavelet shrinkage to reduce noise. The result is shown as the black curve, and the rise time of 10-90% of leading edge is then estimated.

FIG. 36: Illustration of wavelet analysis [60].



A typical tendency between the rising time and energy distribution is presented in Fig.37, where two gatherings are clearly separated. The up part which has longer rising time corresponds to the surface events, so that should be discarded by the red critical line. The down part is then determined to be the final spectrum. Efficiency correction is needed afterwards, which could be estimated by source calibration data.

FIG. 37: Illustration of the surface event cut [61].



VIII. THE PROSPECT

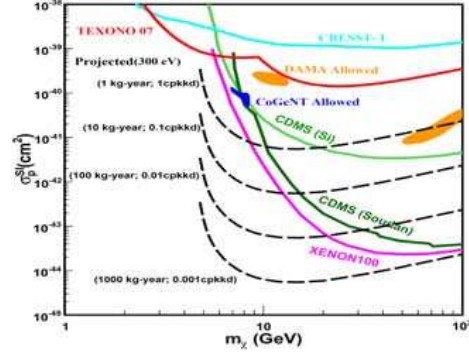
A. Physical target

The CDEX Collaboration will realize the dark matter detection with point-contact germanium arrays as the detector which is cooled down and actively shielded by the liquid argon system. The most interesting region for the CDEX experiment is the low WIMP mass region which could be detected by the ultra-low energy threshold PCGe detector. Based on the performances of the prototype 1 kg PCGe detector which has run for several months in the shielding system at CJPL, the CDEX collaboration plans to focus on the direct detection of dark matter particles with a minimum mass less than 10 GeV. The Ge array system will run in the CJPL and additional shielding system will be included such as 1 m-thick polyethylene for neutron deceleration and absorption, 20 cm lead and 20 cm Oxygen-Free High-Conductivity copper for gamma shielding. A liquid argon cooling and active shielding system will be adopted for the CDEX-10, and the PCGe detector will be immersed into the liquid argon system. The passive and active shielding systems provide the Ge array system a relatively low background circumstance, thus running experiments with low background is expected. Except the shielding system, the effective pulse shape discrimination (PSD) methods will also be developed to get rid of the noise and background events from the raw data and pick up the real dark matter events. These PSD methods mainly focus on (1) the pulse shape analysis of the events near noise-edge to enlarge the observable physics range, (2) the pulse shape analysis of surface events, by comparison with the bulk events one can

characterize the important background channel, (3) understanding the sub-keV background and offering a scheme to suppress it.

By considering all possible effects in the design which might affect the performances of the detector and carrying careful data analysis, we wish to achieve a level of 1cpkkd (count per kilogram per keV per day) for the CDEX-1 stage and 0.1cpkkd for CDEX-10 stage. The different exclusive curves corresponding to different energy thresholds and background event rates are shown in Fig.38.

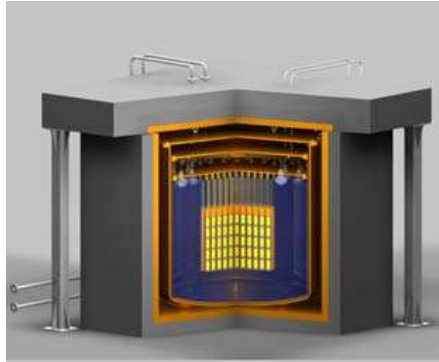
FIG. 38: The different exclusive curves correspond to the different energy threshold and background event rate.



B. CDEX-1T

The ultimate goal of the CDEX Collaboration is to set up a ton-scale mass Ge detector based on the PCGe detector and LAr active shielding and cooling systems. The detailed design and technology which will be developed and utilized are based on the experience and lessons gained from the design and studies of the CDEX-10 detector. The detector will be located in a 1 m-thick polyethylene shielding room and the internal volume is covered by 20 cm lead and 10 cm Oxygen-Free High-Conductivity copper. The threshold less than 400 eV and background event rate of 0.001 count per keV per kilogram target mass per day for the 1 T Ge mass are the main goal of the CDEX-1T detector. The sensitivity for low mass dark matter will be down to about 10^{-45}cm^2 in the region of the WIMP mass less than 10 GeV if the 0.001cpkkd background level is achieved, as shown in Fig.38. The rough layout of the CDEX-1T detector is shown in Fig.39.

FIG. 39: Layout of the CDEX-1T detector system.



IX. SUMMARY

Astronomical observation, especially the cosmic microwave background (CMB) radiation and the data on the large scale structure (LSS) of the universe indicate that a significant part of matter content of our universe is non-baryonic

dark matter. The nature of the dark matter is one of fundamental problems of particle physics and cosmology. A favored candidate of the dark matter is the WIMPs, weakly interacting massive particles. Direct searches of the WIMPs are aiming at detecting the interaction of WIMPs with normal nuclei which are SM particles. The CDEX (China Dark matter Experiment) collaboration is a new experimental group for searching dark matter in the world whose task is to directly search for WIMP with an Ultra-low energy threshold in terms of high purity Germanium detector at CJPL (The China Jin-Ping deep underground laboratory). So far, the CDEX collaboration includes several members: Tsinghua university , Sichuan university , Nankai university, Institute of Atomic Energy, Yalong River Basin Company and Nuctech Company.

The CJPL is located in the central portion of one of the transport tunnels of a giant hydrodynamic engineering project at the huge Jin-Ping Mountain area of Sichuan province, southwest of China. The rock covering thickness of CJPL is about 2400 m where the cosmic muon flux is about 1 in 10^{-8} of the ground level. The Muon flux, radioactivity and radon concentration in the underground lab have been measured and monitored time to time.

Comparing the detectors made of other materials the high purity Germanium semi-conductor detector HPGe has many advantages such as low radioactivity, high energy resolution, high density and remarkable stability for radiation detection. The CDEX adopts the high purity point contact Germanium detector PCGe with about 300 eV threshold to search for WIMPs of minimum mass as low as 10 GeV. The detector mass of first phase CEDX1 is 1 Kg and that of second phase CDEX10 is 10 kg.

There are two detectors of CDEX1, 20 g HPGe and 1 kg PCGe, running now in the CJPL. The detector surrounded by CsI(Tl) or NaI(Tl) veto detector and outside the veto detector there is a shielding system. The performance of the detector has been calibrated and the noise level is about 200 eV. The expectation of background count is less than 0.1cpd/keV/kg near the 200 eV after event selection with the PSD cut, noise edge cut and wavelet cut.

The CDEX-10 is a PCGe detector array which is immersed into a liquid Argon (LAr) vessel. Each unit detector in the array is a 1 kg PCGe detector whose threshold is about 200 eV. The scintillation light in the LAr will be read out by the PMT, and the LAr is the cooling system providing working temperature for the Ge detector and also serves as a veto detector. The Monte-Carlo study shows that the background event rate will be as low as 1cpd at low energy range. In the future, the CDEX Collaboration is going to set up a ton-scale Ge detector composed of the PCGe detector and LAr active shielding and cooling system in the CJPL. Hopefully, the overall threshold of the CDEX-1T detector will be less than 400 eV and the background event rate could be reduced to 0.001 cpd. The sensitivity will be down to about 10^{-45}cm^2 for the WIMP with its minimum mass as low as 10 GeV or even less.

Acknowledgements:

This work is partly supported by the National Natural Science Foundation of China (NNSFC); Ministry of Science and Technology of China (MOSTC) and Ministry of Education of China.

-
- [1] F. Zwicky, *Astrophys. J.* **86**, 217(1937).
 - [2] V. Trimble, *Ann. Rev. Astron. Astrophys.* **25**, 425(1987).
 - [3] E. W. Kolb and M. S. Turner, ‘the Early Universe’ (Addison-Wesley, Reading, MA, 1990).
 - [4] L. Bergstrom, *New J. Phys.* **11**, 105006(2009)[arXiv:0903.4849 [hep-ph]].
 - [5] J. L. Feng, arXiv:1003.0904[astro-ph.CO] (2010); R. J. Gaitskell, *Ann. Rev. Nucl. Part. Sci.* **54**, 315(2004).
 - [6] X. He et al. *Mod. Phys. Lett.* **A22**, 2121(2007); *Phys. Rev.* **D79**, 023521(2009).
 - [7] A. Beylyayev et al. *Phys. Rev.* **D83**, 015007(2011), and the references therein.
 - [8] H. An, S.-L. Chen, R. N. Mohapatra, S. Nussinov and Y. Zhang, *Phys. Rev.* **D82**, 023533(2010) [arXiv:1004.3296 [hep-ph]].
 - [9] M. Gilloz et al. *JHEP* **1103**, 048(2011), and references therein.
 - [10] J. Lavalle et al, *AIP Conf.Proc.* **24**, 398(2010); R. Yang and J. Chang, *Res.Astro.Astrophys.* **10**, 39(2010), and references therein.
 - [11] Tibet ASgamma Collab. *Astrophys. Space. Sci. Trans.* **7** 15.
 - [12] K. Bernabei et al. *Eur. Phys. J.* **C56**, 333(2008); *ibid.* **C67**, 39(2010).
 - [13] C. Aalseth et al. *Phys. Rev. Lett.* **106**, 131301(2011).
 - [14] P. Brink et al. *AIP Conf.Proc.* **1182**, 260(2009).
 - [15] The CROSST-collab. arXiv: 1109.0702.CRESST
 - [16] G. Jungman, M. Kamionkowski, K. Griest. *Phys. Rept.* **267**, 195(1996)[arXiv:hep-ph/9506380].
 - [17] C.-L. Shan, arXiv:1103.4049 [hep-ph].
 - [18] C.-L. Shan, arXiv:1103.0481 [hep-ph].
 - [19] H.Y. Cheng et al. *Phys. Lett. B* 219, 347 (1989); *JHEP* 07, 009 (2012) [arXiv:1202.1292].
 - [20] R. Essig, J. Mardon and T. Volansky, *Phys.Rev.* **D85** (2012) 076007; R. Essig et al. *Phys.Rev.Lett.* **109** (2012) 021301.
 - [21] T. Ressel, M. Aufderheide, S. Bloom, K. Griest and G. Mathews, *Phys. Rev.* **D48**, 5519(1993).

- [22] G. Griest, Phys.Rev.**D15**, 2357(1988).
- [23] V. Barger, W.-Y. Keung and G. Shaughnessy, Phys. Rev. **D78**, 056007(2008) [arXiv:0806.1962 [hep-ph]].
- [24] Y. Tzeng and T. T. S. Kuo, Conference: C96-05-22, 479.
- [25] M. T. Ressell *et al.*, Phys. Rev. **D48**, 5519(1993).
- [26] M. T. Ressell and D. J. Dean, Phys. Rev. **C56**, 535(1997); hep-ph/9702290.
- [27] J. Ellis, K. Olive and C. Savage, Phys. Rev.**D77**, 065026(2008).
- [28] R. Helm , Phys. Rev.**104**, 1466(1956).
- [29] I. Sick, Nucl. Phys. A **218**, 509(1974).
- [30] Dreher *et al*, Nucl. Phys. A **235**, 219(1974).
- [31] J. D. Lewin and P. F. Smith, Astropart. Phys.**6**, 87(1996).
- [32] Y.-Z. Chen, Y.-A. Luo, L. Li, H. Shen and X.-Q. Li, Commun. Theor. Phys. **55**, 1059(2011); [arXiv:1101.3049 [hep-ph]].
- [33] J. Engel, S. Pittel and P. Vogel, Inter. J. Mod. Phys. **V1**, 1(1992).
- [34] J. Engel, Phys. Lett. **B264**, 114(1991).
- [35] J. D. Walecka, Muon Physics, Vol. 2, ed. V. W. Hughes and C. W. Wu (Academic Press, New York, 1975), p. 113
- [36] M. Cannoni, arXiv: 1108.4337; J. O’Connell, T. Donnelly and J. Walecka, Phys. Rev. **C6**, 719(1972); V. Bednyakov and H. Klapdor-Kleingrothaus, Phys.& Nuclei **40**, 583(2009); C. Shan, arXiv:1103.0482; V. Bednyakov and F. Simkovic, arXiv:0406218; M. Ressell *et al.* Phys. Rev. **D48**, 5519(1993); V. Bednyakov, arXiv: 0310041; G. Belanger *et al.* Computer Phys.Commun. **180**,747(2009); and many other authors.
- [37] T. Donnelly and W. Haxton, Atomic Data and Nuclear DATA Tables **23**, 103(1979).
- [38] R. Bernabei *et al.*, Eur. Phys. J. **C67**, 39(2010)R. Bernabei *et al.*, Prog. Part. & Nucl. Phys. **66**, 169(2011).
- [39] KIMS Collaboration Phys. Rev. Lett. **99**, 091301(2007).
- [40] www.sciencexpress.org /11 February 2010/Page 3/10.1126/science.1186112; XENON Collaboration, Phys. Rev. Lett.107, 131302 (2011).
- [41] Yue Qian, Cheng Jianping, Li Yuanjing, *et al.* HEP & NP **28**, 877(2004); LI Xin, YUE Qian, *et al.*, HEP & NP, **31**, 564(2007).
- [42] TEXONO Collaboration, Phys. Rev. **D79**, 061101(R)(2009).
- [43] CoGeNT Collaboration, Phys. Rev. Lett. **106**, 131301 (2011); Phys. Rev. Lett. 107, 141301 (2011).
- [44] For more information, see <http://www.npl.washington.edu/majorana/>
- [45] For more information, see <http://www.mpi-hd.mpg.de/gerda/>
- [46] Topics in Astroparticle and Underground Physics (TAUP 2009) , Journal of Physics: Conference Series 203 (2010) 012028 doi:10.1088/1742-6596/203/1/012028
- [47] SCIENCE , 5 JUNE, **324**, 1246(2009).
- [48] G. Heusser, Ann. Rev. Nucl. Part. Sci. **45**, 543(1995).
- [49] Canberra, <http://www.canberra.com/>
- [50] Chinalco Luoyang Copper Co., Ltd, <http://www.lycopper.cn>
- [51] S. T. Lin, H. B. Li, X. Li, *et. al* , Phys. Rev. D79, 061101(R)(2009).
- [52] P. N. Luke, F. S. Goulding, N. W. Madden, *et. al.*, IEEE Tran. Nucl. Scie, **36**, 926(1989).
- [53] P. S. Barbeau, J. I. Collar, O. Tench, J. Cosmo & Astropart Phys. (JCAP) **09**, 009, 1(2007).
- [54] www.amptek.com
- [55] www.tek.com
- [56] cdms.berkeley.edu
- [57] xenon.astro.columbia.edu
- [58] www.cresst.de
- [59] C. Aalseth *et al.*,Phys. Rev. Lett.**107**, 141301(2011).
- [60] M. G. Marino, (2010) Ph. D. dissertation, Univ. of Washington, 263.
- [61] From a talk given by J. F. Wilkerson in Tsinghua university in 2011.